TRACE ELEMENT GEOCHEMISTRY OF FLOWBACK BRINES FROM THE MARCELLUS SHALE

Research Thesis

Submitted in partial fulfillment of the requirements for the graduation with research distinction in Earth Sciences in the undergraduate colleges of The Ohio State University

By

Benjamin D. Holt
The Ohio State University
2016

Approved by

Thomas H. Darrah, Advisor
School of Earth Sciences

TABLE OF CONTENTS

Abstract

Hydraulic fracturing has become a popular and widely successful method of recovering oil and natural gas from unconventional resources, particularly shales. As hydrocarbons are recovered from black shales, flowback fluid consisting of formation brines and hydraulic fracturing fluids are brought to the surface. The fluids are typically hypersaline and often rich in trace and heavy metals and radionuclides. For this reason, flowback fluids and formational brines are an important area of study as many of these trace elements are toxic environmental pollutants (barium, arsenic, etc.), while others, such as rare earth elements (REE's) and platinum group elements, have potential economic viability. Despite the importance of brines, analysis of their trace metals remain difficult by current analytical methods due to relatively low metal concentrations, high concentrations of dissolved solids and salts, and a lack of matrix matched analytical standards. Therefore, the objective of this project was to develop a robust analytical method for evaluating alkali metals, rare earth elements, lanthanides, and actinides in flowback brines with high total dissolved solids, salt content, and organic contents. To do this, I analyzed flowback samples from wells within the Appalachian Basin, commonly produced from the Marcellus Formation, by inductively coupled plasma mass spectrometer (ICP-MS). Two methods were used to reduce the total dissolved solid and salt concentrations. First, we used a commercial resin to remove salts, which proved unsuccessful. Second, we successfully tried dilution then analysis by ICP-MS of trace element concentrations to a part per trillion level (but still well above ICP-MS detection limits). The results of this project included a sensitivity analysis of the measured elements by concentration. By so doing, these data revealed the viability of this method to get accurate and precise results for the majority of the analytes measured. Additionally, concentrations of rare earth elements and actinides were be compared to their average crustal and oceanic concentrations to provide a geological context for the occurrence of these elements. These plots revealed REE enrichment patterns that are expected by the marine black shale depositional setting of the Marcellus shale, and thus underscored the ability of the dilution method to make geologic interpretations from resultant brine element concentrations.

ACKNOWLEDGEMENTS

I acknowledge financial support from NSF EAGER (EAR-1249255) and NSF SusChem (EAR-1441497) to my advisor Thomas Darrah. I thank Professor Avner Vengosh (Duke) for providing access to samples and for stimulating discussions on the hydrogeology and geochemistry of brines. I also acknowledge the Shell Exploration and Production Company for the opportunity and funding that made my participation in this project possible. Additionally, I am deeply thankful for the assistance with experimental design, access to instrumentation, and guidance throughout this project provided by Dr. John Olesik, Anthony Lutton, and Dr. Thomas Darrah. I also am grateful for for the invaluable patience, expertise, editing, and guidance that Dr. Anne Carey has provided me throughout this process. Finally, thank you to my mom, my dad, my sister, my best friends for their love and support since the beginning.

LIST OF FIGURES

LIST OF TABLES

INTRODUCTION

In recent years, horizontal drilling and hydraulic fracturing innovations have dramatically increased the ability to tap unconventional hydrocarbon resources from shales and other tight formations, and have propelled the United States to become the top natural gas producer globally (Kerr, 2010). Pennsylvania's Marcellus Shale, located in the Appalachian Basin has played a large role in this shale-gas boom, as it is the site of more than 8500 unconventional shale wells (Brantley et al., 2014; Howarth et al., 2011; Kerr, 2010). This production boom has been coupled with growing public concern about the environmental impact of hydraulic fracturing, especially in relation to groundwater quality (Brantley et al., 2014; Jackson et al., 2014; Vengosh et al., 2014; Vidic et al., 2013).

However, to understand the purpose and context of this project, it is imperative to have an understanding of the hydraulic fracturing process and how brines are defined and travel through the stages of hydraulic fracturing. Five primary stages of water use throughout the hydraulic fracturing process have been identified to summarize the production and role of flowback fluids (Briskin, 2015; Jackson et al., 2014; Vengosh et al., 2014; Vengosh et al., 2013). (1) water is gathered from some reservoir (e.g., creeks, ponds, rivers, ground water) for use in hydraulic fracturing (Jackson et al., 2014; Kondash and Vengosh, 2015); (2) at the well site, the water is mixed with the production company's proprietary chemical mixture that includes surfactants, acids, proppants, biocides, and other chemicals (Briskin, 2015); (3) fluids are injected into the well at high pressures to induce fractures within the target rock formation (typically shale) (Briskin, 2015; Ellsworth, 2013); (4) the water and chemical blend mixes with subsurface formational brines, which is subsequently returned to the surface following the onset of production, where it is sequestered and managed by the production company (Briskin, 2015; Drollette et al., 2015; Vengosh et al., 2014); (5) finally, the flowback may be treated, reused, or injected into wastewater wells (Briskin, 2015; Ellsworth, 2013; Haluszczak et al., 2013; Harkness et al., 2015; Rahm et al., 2013; Vidic et al., 2013).

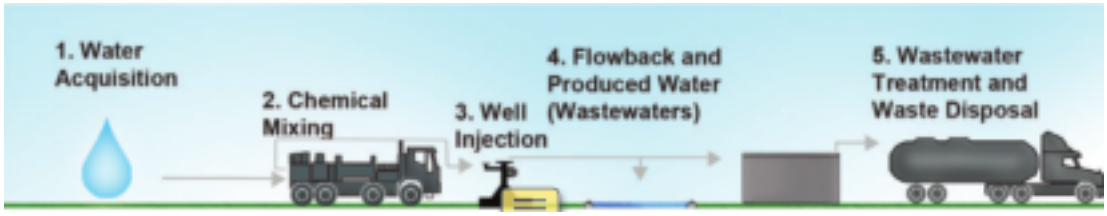

Figure 1. Overview of water use throughout the hydraulic fracturing process (Brisken, 2014).

Furthermore, recent studies have identified over 1000 chemical compounds that are commonly present in fracking fluids with several of these being toxic solutions (e.g., Drollette et al., 2015). Additionally, recent studies have determined that flowback brines from Marcellus shale-gas plays may exhibit salinities up to 300,000 mg/L (Parker et al., 2014; Rahm et al., 2013; Vengosh et al., 2014; Warner et al., 2013; Warner et al., 2014; Warner et al., 2012). This knowledge, combined with the immense volumes (~more than a billion gallons per year) of this flowback fluid came back to the surface at Marcellus shale-gas wells in Pennsylvania (Kondash

and Vengosh, 2015; Rahm et al., 2013; Vengosh et al., 2014), further exacerbates public concern about the composition of flowback fluid. The EPA has even recently identified the development of analytical methods to better quantify the chemical composition of flowback brines as a primary goal of recent projects (Briskin, 2015).

Therefore, the goal of this project is to address increased public interest in the chemical composition and potential environmental impacts of flowback fluid by developing and validating analytical techniques using SPR-IDA chelating resin and sample dilution for analyzing flowback brines. In particular, we developed ICP-MS brine analysis methods for rare earth elements, actinides, lanthanides, and various other elements. We then assessed method viability for different suites of elements while also using the data to make statements about the composition, source, and environmental implications of these flowback fluids.

GEOLOGIC SETTING

Marcellus Formation Geologic Overview

The Northern Appalachian Basin (NAB) is a regional sedimentary basin that extends from New York, through Pennsylvania and West Virginia, and into Eastern Ohio and Kentucky. The formation of this foreland basin occurred as a direct result of sediment deposition and structural deformation associated with the Taconic, Acadian, and Alleghenian orogenies (Faill, 1997a, b, 2011; Sak et al., 2012; Scanlin and Engelder, 2003).

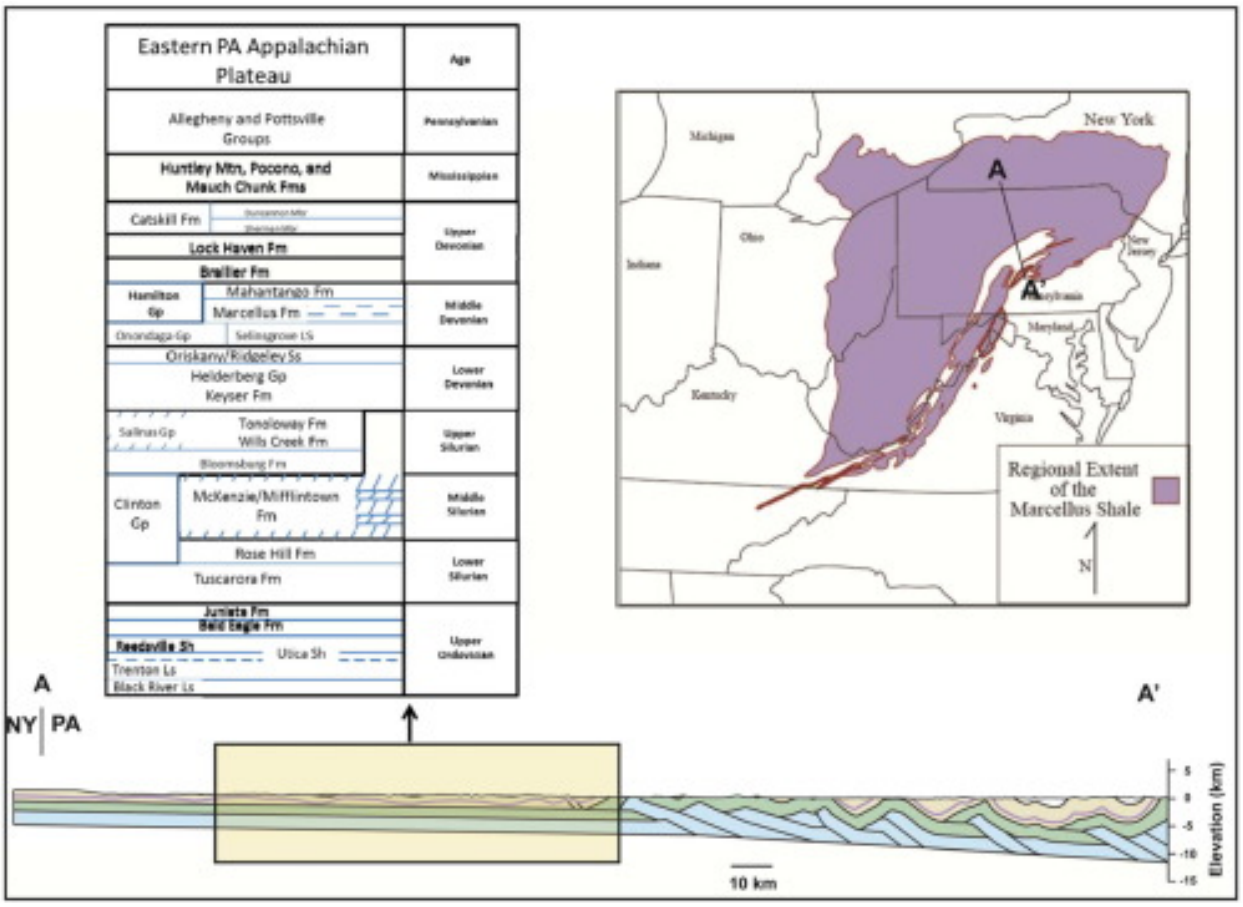

Figure 2. A generalized stratigraphic column (left), areal extent of the Marcellus Formation (right), and a simplified structural cross-section (reproduced from Sak et al., 2012 and Darrah et al., 2015a) of the northern Appalachian Basin (NAB) plateau in northeastern PA and southern NY (bottom, see cross-section A–A′ on map). The Marcellus Formation outcrop belt (upper right) is highlighted in red and the areal extent of the Marcellus Formation is shown in purple. The generalized structural cross-section (bottom) spans from the Appalachian Plateau (to the north and west) to the intensely deformed Valley and Ridge province (southeast) across the Appalachian Structural Front (ASF) (Darrah et. al 2015a).

The Hamilton Group is the Middle Devonian sedimentary sequence that includes the Marcellus Formation. The Hamilton Group was initially deposited as a wedge of marine sediments that thickens to the southeast of the Alleghenian structural front. The Marcellus Formation itself forms the basal member of this Hamilton Group and is composed dominantly of organic-rich and siliclastic black shales (Ryder et al., 1996; Straeten et al., 2011). Past studies have utilized Rb-Sr dating to determine that the Marcellus was deposited approximately from 384 ± 9 to 377 ± 11Ma (Bofinger and Compston, 1967). The dominant period of deformation of the Marcellus occurred as the Hamilton Group slid by "salt tectonics" atop the Salina Formation and along the Appalachian Plateau detachment surface (Lash and Engelder, 2009, 2011; Scanlin and Engelder, 2003). This Alleghenian deformation, together with clastic loading and thrust-load-induced subsidence, buried the Hamilton Group to depths that effectuate diagenesis and catagenesis of the Marcellus Formation (Evans, 1994, 1995; Evans and Battles, 1999; Lash and Engelder, 2009). See Darrah et. al., (2015) for a more comprehensive survey of the depositional and deformational history of the NAB. The samples for this project were taken from shale-gas wells in the Pennsylvania and New York sections of the Marcellus Formation.

METHODS

The presence of brines 1 to 4 times the salt and total dissolved solid (TDS) content of seawater presents significant analytical challenges for determining the concentration of major (e.g., Ca, Mg, Na), minor (e.g., Sr, Ba, Fe) and trace elements (e.g., REE's, U, Th, As) in flowback and formational brine samples. As a result, herein we describe the two methods of sample preparation we used in order to conduct these measurements. These methods include the use of a commercially available resin designed to remove NaCl and dilution to reduce the total dissolved solid content of the sample.

Sample Collection

The flowback and formational brine samples included in this study were collected from well sites across the Marcellus Formation in Pennsylvania and New York. As part of previous studies, these samples have been analyzed for major cations and anions (e.g., Cl, Br, Na, K), water isotopes ($\delta^{18}O$-H_2O; $\delta^{2}H$-H_2O), strontium concentrations and strontium isotopes ($^{87}Sr/^{86}Sr$), gas composition (C_1 to C_5 hydrocarbons, N_2, O_2, H_2, CO_2) and noble gases (He, Ne, Ar, and their isotopes) (Darrah et al., 2015a; Darrah et al., 2015b; Darrah et al., 2014; Warner et al., 2014; Warner et al., 2012).

Before sampling, actively pumping shale-gas wells were purged through stainless steel sample tubing to flush sampling lines and remove stagnant water until stable values for pH, electrical conductance, oxidation-reduction potential, and temperature were obtained following methods reported previously (Osborn and McIntosh, 2010; Osborn et al., 2012; Warner et al., 2012). Water samples were collected prior to any treatment systems or pressure tanks following standard methods for water samples (USGS, 2011).

Sample Preparation and Analysis

All hydraulic fracturing flowback and formational brine samples (n=50) were analyzed for Ca, and their minor and trace elements by inductively coupled plasma mass spectrometry by standard analytical methods for inductively coupled plasma mass spectrometry (Cuoco et al., 2013; Darrah et al., 2015a; Darrah et al., 2015b; Darrah et al., 2014; Thomas, 2003; Warner et al., 2014; Warner et al., 2012) using a Thermo Finnigan Element 2 ICP-MS. Sample preparation methods were varied to optimize the methods. These methods, as mentioned above, include include the use of a commercially available resin from Teledyne CETAC Technologies designed to remove salt and dilution to reduce the total dissolved solid content of the sample.

Method 1. Commercially available resin to remove the salts

The first method developed to analyze the flowback fluids utilized CETAC SPR-IDA (suspended particle reagent iminodiacetate). This product is a commercially available resin that may be utilized to concentrate trace elements for analysis by reducing high alkali metal contents (Jerez et. al, 2013). The brine samples analyzed in this study are highly enriched in Na and therefore, without reducing the amount Na in the sample solution, this extreme Na signal will suppress trace element signals and cause spectral overlap due to polyatomic ions. The product was initially designed to reduce saline matrix of seawater samples to enhance detection of trace elements. The goal of this method development was to apply the same technique to more saline flowback samples.

First of all, the viability of this method was tested by creating a seawater imitation

solution based on using seawater reference solution CASS-4 from the National Research Council (Canada). This CASS-$ imitation solution consisted of multi-element calibration standards ICP-MS-68 Solution A and B (commercially available from High Purity Standards) diluted to 0.5ppb, 10,000ppm Na, 1,000ppm Mg, 300ppm Ca, 2% nitric acid, and water purified to 18.2MΩcm (by Milli-Q purification system) to mimic the composition of the CASS-4 seawater reference. Thus, SPR-IDA could be tested on a solution representing seawater before applying the resin to our flowback samples.

A blank solution was made by diluting a 40mL nitric acid aliquot and a 2.04 mL 10,000ppb In and Bi solution to 2.0L using purified water. Five solutions were prepared using 10mg/L multi-element calibration standards ICP-MS-68 Solution A and B obtained from High Purity Standardsfor use as external standards. The concentrations of the analyte elements in these standards were 0.1, 1, 10, 50, 100 ppb for standards 1-5 respectively.

The samples for this procedure consisted of 15mL of the above seawater imitation solution, a 100µL aliquot of the SPR-IDA resin, and 45µL of concentrated pure 15.9 molar NH_4OH (ammonium hydroxide). Ammonium hydroxide was added to all samples in order to adjust the pH to the ideal operational acidity of the SPR-IDA resin (approximately 8.0). In this basic environment, the resin is designed to absorb trace elements.

After sample preparation was completed by adding the 100µL SPR-IDA aliquot to 125 mL HDPE sample bottles, each sample was swirled thoroughly and then centrifuged at 1000 rpms for ten minutes. The allows the SPR-IDA beads to consolidate at the bottom of the sample vial so that the supernatant liquid was carefully poured off thus removing the saline matrix. Next, each sample was re-acidified using a 7% HNO_3 (nitric acid) solution. The SPR-IDA resin releases the bound trace element analytes in the acidic environment created by the addition of nitrice acid (i.e., acidified to a pH of 1). Finally, the samples were diluted to 30mL with purified water.

The Thermo Finnigan Element 2 was calibrated using the 5 standards and the blank to create a simple linear regression calibration curve for each analyte. Each “seawater imitation” sample was analyzed by the instrument using this calibration.

Method 2. Sample Dilution

Sample, Standard, and Blank Preparation

To reduce salt and total dissolved solid (TDS) content in the brine sample matrix, each sample was diluted by a factor of 200. These diluted samples were made by first pipetting a 0.5mL aliquot of the flowback fluid and a 2.0mL aliquot of concentrated pure 15.9M HNO_3. Next each sample was diluted to 100.8g using water purified to 18.2MΩcm (by a Milli-Q purification system). This results in each sample solution of 0.5% flowback fluid and 2% nitric acid (by volume). Finally, a 0.1mL aliquot of a 10,000 part per trillion (ppt) indium (In) and bismuth (Bi) solution was added to each sample solution to act as an internal standard, which can be utilized to monitor and correct for instrumental drift (Darrah et al., 2009; Thomas, 2003). Certified multi-element seawater reference solutions NIST 1643e and TMDA-64.2 were diluted by a factor of 200 using the same method. In this way, these multi-element solutions of known concentration may be used as a check of instrument drift throughout analysis.

Five solutions were prepared using 10mg/L multi-element calibration standards ICP-MS-68 Solution A and B for use as external standards using the above method. The concentrations of

analyte elements in these standards were 1, 10, 25, 100, 1000 ppt for standards 1-5 respectively. As demonstrated later, these standards are used to create external calibration curves for each element before analysis.

An additional large blank solution was made by diluting a 40mL nitric acid aliquot and a 2.04 mL 10,000ppt In and Bi solution to 2.0L using purified water. This large blank batch allows for frequent cycling of clean blanks throughout analysis to reduce error contributed by blank contamination over time.

Instrument Calibration and Sample Analysis

The Thermo Finnigan Element 2 ICP-MS was calibrated using five external standards (closely following the method described by Thomas, 2003). This method generates a weighted linear regression calibration curve for each analyte mass using known concentrations of each standard and ion intensity (counts per second) (Figure 2). Internal standards of In and Bi, at the same concentrations as in the blanks and unknown samples, were used in addition to the external standards. As analysis proceeds, changes in In and Bi concentrations are interpreted as similarly occurring to the analytes of intests. Thus, the analyte concentration measurements are corrected by these changes in measured internal standard concentration (Thomas, 2003; Darrah et al, 2009; Warner et al, 2012).

The 50 samples were analyzed over the course of three different days. Blanks, standards, and samples were analyzed with three replicates. The blank solution was run for two minutes between analysis of any standard, blank, or sample in order to reduce memory effects and to wash the sample intake tubing. After calibration for each of these runs, the 100 and 10 ppt standards, a fresh blank, and the diluted NIST and TMDA solutions were all run as samples to check the accuracy of the calibration. Next, samples were analyzed in sets of approximately seven. After this, the diluted NIST solution and a fresh blank were analyzed to check for instrument drift.

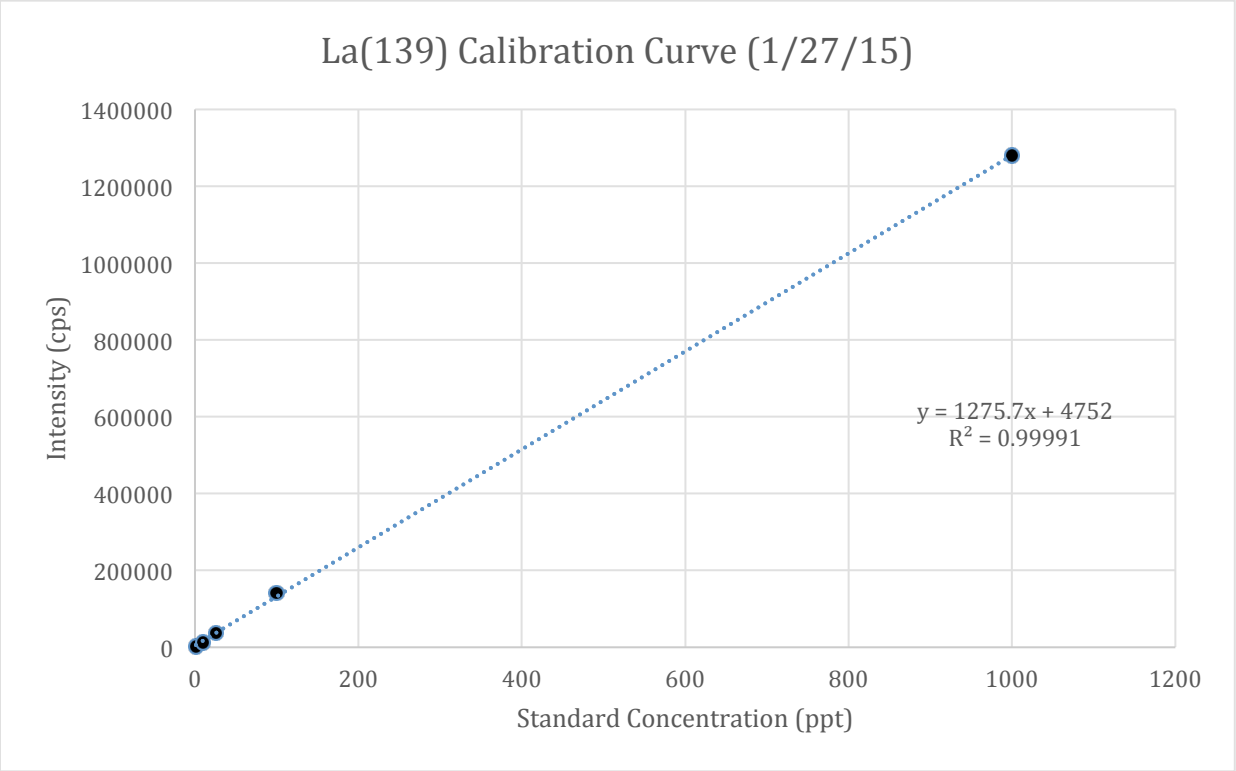

Figure 3. Example of calibration using external standards to generate a linear regression.

RESULTS

A comparison of preparation methods

At the beginning of this project, we were optimistic that the SPR-IDA method would be effective. The method which utilizes SPR-IDA does not dilute of analytes of interest, but actually preconcentrates the analytes. However, when testing this method, the element signal expected from the known concentration of elements in the "seawater imitation" samples was reduced greatly. Degree of element retention varied by analyte, but all elements of interest were reduced by at least 90%.

In an attempt to reduce the degree of element loss in the samples, subsequent tests using the SPR-IDA beads were re-run while carefully checking and adjusting the pH with nitric acid additions at every stage of the method. Additionally, separate tests with and without Na spikes were run in order to see if the salinity was affecting analytical capability. Despite these attempts to improve element recoveries, the results were persistent and the cause of elements being washed out was not conclusively determined.

However, by the dilution method, the majority of the suite of elemental analytes was consistently above detection limits. Therefore, the ability to get data from the samples by the dilution method indicates that dilution by a factor of 200 generally does not weaken analyte signal to the point that it is below detection limits. This method still resulted in some analytical challenges for certain elements, particularly spectral overlap due to polyatomic ions. Yet, overall, dilution proved to be the more effective method for analysis of flowback brines by ICP-MS.

Concentration of major elements

The elemental data from this project are presented in Appendix 2(A-E) and the correlation matrix for these data is presented in Appendix 1 (A-H).

Table 1 displays the elemental abundance of each analyte, shown according to the mass measured for each Marcellus flowback sample in parts per trillion (ppt). All concentration values presented in Table 1 have been multiplied by a factor of 200 to account for the dilution described in the Methods section. As seen in Appendix 2(A-E), several elements are frequently outside an acceptable range of values. These data can be used to infer potential problem analytes in this methodology and to understand why these elements may not be effectively analyzed by this method.

Blank and baseline corrected values that were below detection limits for a given element are denoted as "bdl" for below detection limit. The majority of the elements which were frequently below their respective detection limits included transition metals, specifically Sc, V, Ni, Co, Cu, and Ag. Of the REEs, only Gd and Er were commonly measured as at or below 0 ppt. The only other element below the respective detection limit for many of the samples was Th.

Concentration values that were determined as > 1x 10^{12} parts per trillion (ppt) indicates that sample intensities exceeded the range of the analytical detector and are thus labeled above quantitation limit or "aql" in Table 2. Calcium and aluminum are the two elements in this dataset which are commonly above quantitation limits, which is expected due to their high natural abundance. These elements should be analyzed at higher dilutions (e.g., ~1000x) or with

alternative analytical instruments (e.g., ICP-optical emissions spectroscopy or ion chromatography).

However, all other analytes are comfortably within the analytical range for each respective element on the ICP-MS used in this work. Boron and uranium as well as the remaining transition metals and the REEs all fell within the respective analytical range for each element for the vast majority of samples.

Sensitivity analysis

Based on our analytical data, we plot the concentration range of elements determined as part of this analysis in Figure 3. These data provide a range for the sensitivity and dynamic analytical range for analytes measured by this method.

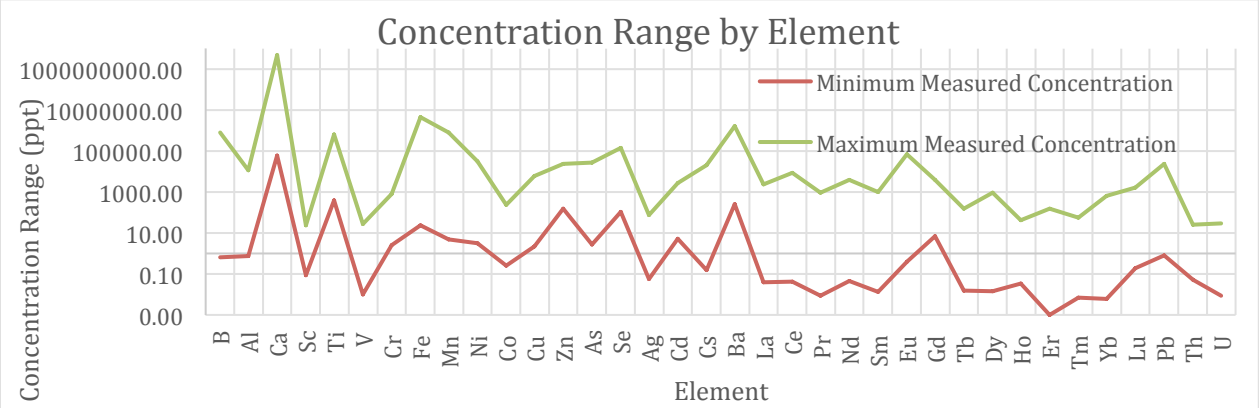

Figure 4. Maximum and minimum concentration of each element measured by dilution method

Of the elements that can commonly be measured above detection limits, the range of concentrations varies greatly. I mention a few examples for illustrative purposes. Arsenic ranges from 2.640ppt-27,290ppt. Barium, another toxin enriched in flowback, exhibits concentrations from 255ppt-1.68 x 10^6 ppt. The REEs tend to display smaller ranges of only a few thousand ppt, such as lanthanum which ranges from 0.04ppt-2330ppt. Uranium concentrations have some of the least variation in this data set, only ranging between 0.01ppt-29.9ppt.

Correlation Matrix

Appendix 1(A-H) presents the correlation matrix for each analyte and the r^2 (numerical estimate of the tightness of correlation fit) and p-values (statistical significance of linear fit). In all cases, p-values of less than 0.05 are deemed significant herein and are highlighted in green. The primary trends of these matrices reveal several strong correlations between different elements and/or suites of elements, including boron, actinides, and REEs. Additionally, the transition metals are largely correlated strongly to each other.

Accuracy and Precision

Table 1 presents the known concentration of measured elements in a 200x NIST 1643e standard in the second column. The following columns present the measured concentrations from this same solution after every 10 samples were analyzed. The majority of the samples in the project were measured on 1/27/15 and thus there are four NIST 1643e standard checks from this date. A comparison of these checks (columns 3-8) to the known concentration of a 200x dilute NIST1643e (column 2) shows the accuracy of these checks. Similarly, the change in measured concentrations over the checks reveals the precision for each analyte.

Element	Nist1643e 200x Actual	11/12/14 A	11/4/14 A	1/27/15 A	1/27/15 B	1/27/15 C	1/27/15 D	Avg Error	Avg Std Dev
	(ppt)	(ppt)	(ppt)	(ppt)	(ppt)	(ppt)	(ppt)	(%)	(ppt)
Ag	5.31	3.92	3.68	3.18	2.99	3.07	3.31	36.8	0.37
Cd	32.84	37.94	49.15	29.74	46.9	58.75	40.78	36.75	10.03
Ba	2721	3432	3316	2883	3940	3506	3802	27.89	374.6
Pb	98.15	94.65	97.31	91.5	98.61	118.9	118.2	8.872	12.14
B	789.5	54.56	63.55	955.9	1080	678.1	553.8	47.81	434.3
V	189.3	393.6	346.2	166.3	173.1	136.5	127	45.39	115.5
Cr	102	104	114	100	103	76.3	69.8	12.2	17.4
Fe	490.5	109.6	111.6	396.2	360.2	327.7	487.7	39.08	155.3
Mn	193.5	337.2	397.9	178	189.9	151.5	216.4	37.22	98.96
Co	135.3	276.5	130.8	124.1	129.9	101.3	91.63	29.56	67.64
Ni	312.05	127.6	131.85	282.39	244.32	171.93	166.11	39.956	62.638
Cu	113.8	311.3	107.7	95.73	108.4	89.14	74.5	42.62	89.16
Zn	392.5	-5.398	111.1	369.8	349.2	268.6	265.8	42.29	145.6
As	291.5			299.5	279.7	337.1	274.3	7.084	28.44

Table 1. NIST 1643e 200x dilute standard checks compared to known concentration of elements in a 200x dilute NIST 1643e solution

DISCUSSION

The SPR-IDA chelating resin was ineffective by this analytical method on the CASS-4 seawater imitation solution and thus has not yet been applied to flowback samples. Despite several tests with this methods, analytes were not retained in the sample solutions. Further work needs to be done in order to draw conclusions on what factors led to the majority of the analytes being almost entirely removed by at some point in the method process. The sample solutions may not have been sufficiently acidified after pouring off the supernatant liquid. Inadequate acidification may be related to the extreme buffering capacity, marked by high TDS, electrical conductivity, etc. of the samples themselves. Future analysis of the supernatant liquid will allow diagnosis of which stage of the method is resulting in analyte reduction.

Overall, our preliminary data suggest that the dilution method (i.e., dilued by a factor of 200) was determined to be a suitable method for the analysis of B, U, Pb, several transition metals, and most REE in the majority of samples. The ability to measure these elements consistently within our quantitation limits (Appendix 2) and the correlations between REE's (Appendix 1) reinforces the suitablility of this dilution method. Notable exceptions to this list include Gd and Er, which were below detection limits in several samples. Because we were able to measure the concentrations of these select elements by the dilution method, we were able to make some observations and interpretations about the geochemical data.

However, trying to measure low concentration elements in a fluid matrix that includes extremely high concentrations of elements such as Cl, Br, Na, and K still led to many analytical challenges. This project demonstrated the difficulties in developing one method for such a broad suite of analytes at varying concentrations. As described in the Results section, Ca and Al were commonly above quantitation limits due to their elevated abundance in nature. In contrast, several transition metals, as well as Gd, Er, and Th, were commonly below detection limits. The method could be altered for a larger dilution in order to bring Ca and Al into our analytical range. Greater dilution could improve data quality for elements such as Eu which currently shows interference due to high Ba (barium oxide spectral overlap with Eu) under the current method (see Fig. 4 and 5). However, such a change would simultaneously worsen our analytical capability for those elements already at or near below detection limits, while potentially driving more transition metals and REEs below detection limits. Overall, a reduction in the dilution factor would likely be the most effective change to the current dilution method as it could strengthen our ability to analyze trace elements and transition metals, thus making analysis of Gd, Er, and U/Th ratios more reliable. While this would drive Ca and Al further above detection limits, these elements are of lesser concern regarding their environmental and/or health concerns than Th or REE and can also be readily analyzed by other techniques. Obvious downsides to this approach include increased analytical and sample preparation costs and the need to have larger initial volumes of samples to account for making several solutions at different dilution factors for each sample.

Isotope dilution, based on comparing sample intensities to known concentrations of designated isotope spikes, could potentially minimize the concerns for the effects of spectrtral overlap. These methods could prevent the need for high dilutions factors and prevent more trace elements from falling below detection limits.

A comparison of the measured brine composition to the BATS 15m seawater reference standard for average oceanic REE concentration overall strong enrichment of REEs in brine

samples. The patterns of REE enrichment relative to seawater in our brine samples reveal two superimposed trends which elucidate geologic information about the brine source rocks (Figure 5).

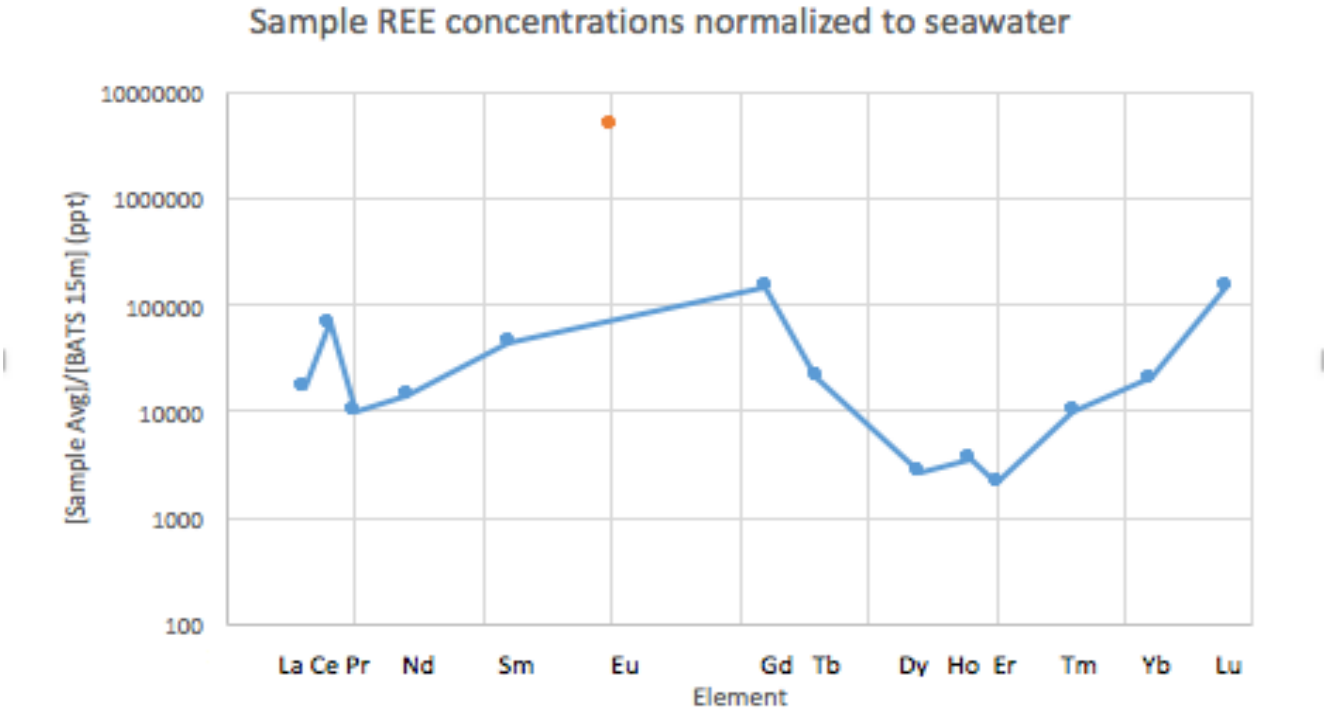

Figure 5. Sample REE concentrations averaged and normalized to BATS 15m seawater standard. Europium plotted as a separate point to illustrate the impact of barium interference.

The first pattern is an overall upward slope of the data. This combined with the enrichment of Ba (measured here) and Sr (published in Warner et al. 2012; 2014) indicate plagioclase feldspar weathering (Warner et al, 2012; Warner et al, 2014). However, the high barium oxide signal causes significant europium interference and so Eu is omitted from the plot. The plagioclase erosional signal is consistent with our picture of the Marcellus basin sediment deposition being fueled by erosion of the continental crust (Taylor and McLellan, 1995; Abanda and Hannigan, 2006). The second trend is often called "high hat," which relates to the enrichment of the middle REEs. Other studies have shown this pattern to be indicative of phosphate weathering. This second pattern also conforms with our understanding of the Marcellus Group as phosphates drive primary productivity and are enriched in black shales (Taylor and McLellan, 1995; Abanda and Hannigan, 2006 Hannigan and Sholkovitz, 2001).

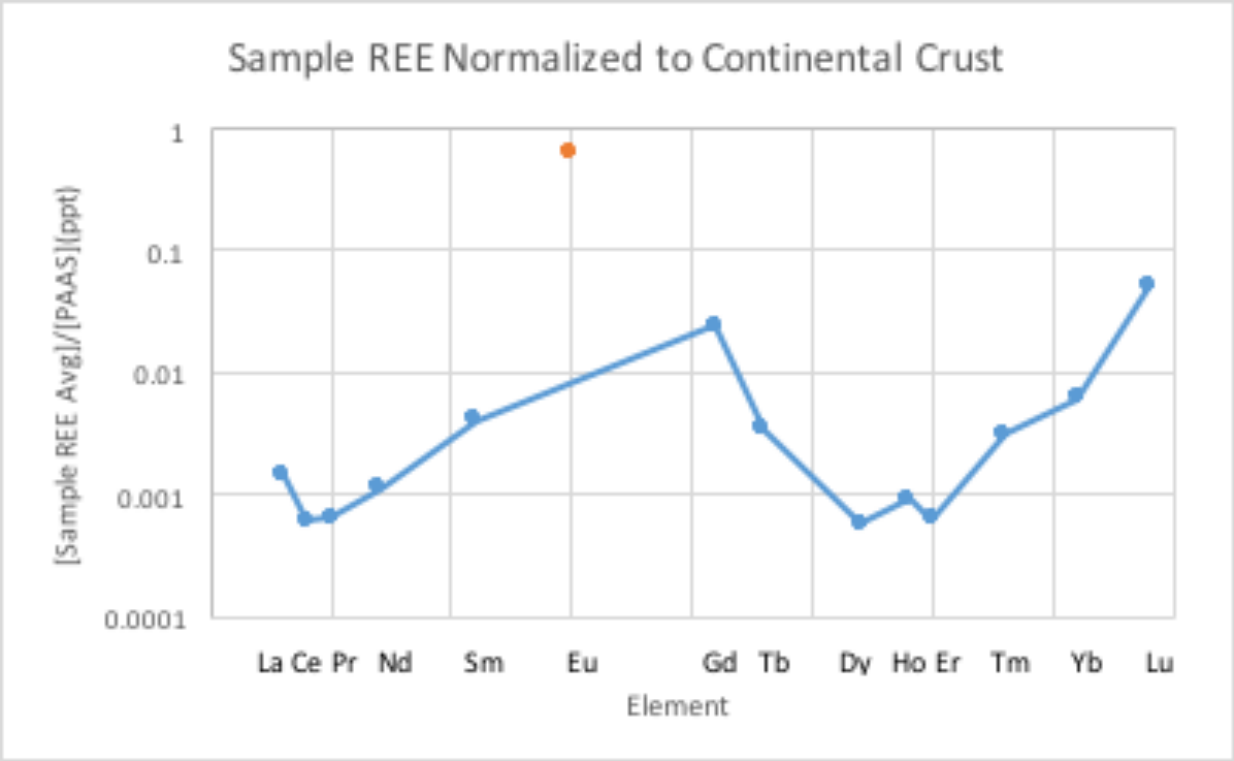

Figure 6. Sample REE concentrations averaged and normalized to PAAS continental crust standard (Taylor and McLellan, 1995). Europium plotted as a separate point to illustrate the impact of barium interference.

Figure 6 demonstrates similar enrichments of REE in comparison to continental crust. Again, high barium concentrations in the brine samples causes europium interference. Thus, Europium plotted as a separate series to illustrate the impact of Barium interference. However, the same observation of an upward slope and MREE enrichment are consistent with plagioclase feldspar and phosphate weathering (Abanda and Hannigan, 2006; Hannigan and Sholkovitz, 2001; Peucker-Ehrenbrink and Hannigan, 2000). Both Figures 5 and 6 exhibit patterns expected from black shale depositional environments with continental crustal erosion (Sagemen et al. 2003; Vine and Tourtelot, 1970; Arthur and Sageman, 1994; and Wignall and Newton, 2001; Wignall, 1991). These consistent results, which are in line with our understanding of the geology of the NAB during black shale deposition, demonstrate the ability of this analytical method to produce viable REE measurements for flowback samples.

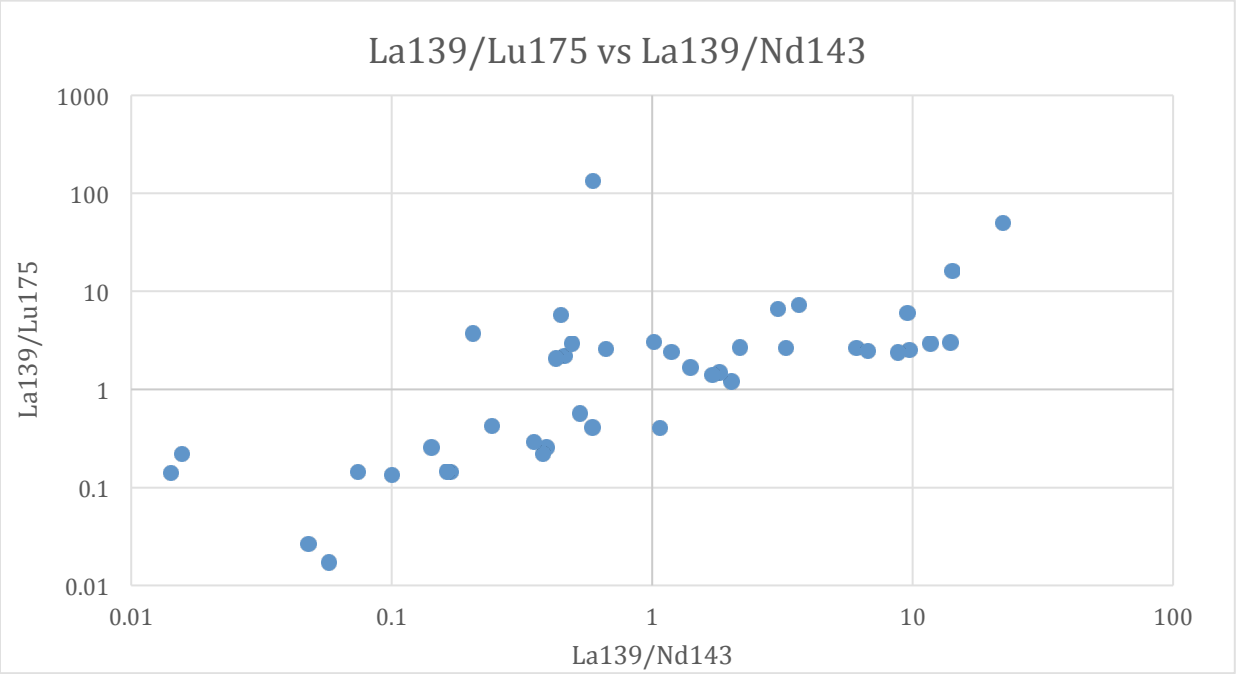

Figure 7. La/Lu vs La/Nd. Low La/Lu shows HREE enrichment compared to LREE. Similarly, low La/Nd shows MREE enrichment relative to LREE. The combination of MREE and HREE enrichments are consistent with the deposition and subsequent water-rock interactions associated with phosphates and plagioclase feldspar.

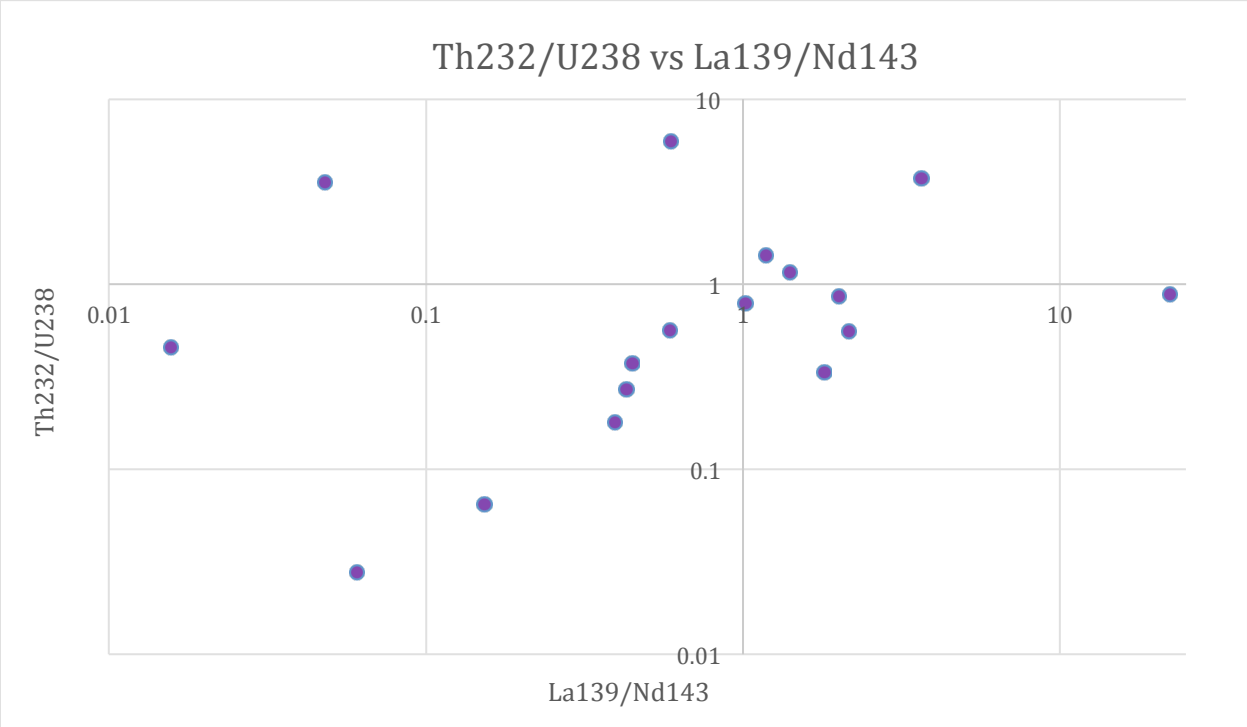

Figure 8. Th/U vs La/Nd. Low Th/U indicates an increasing input of organic-rich sediments in a marine setting, whereas low La/Nd shows MREE enrichment relative to LREE.

Figure 7 reinforces the enrichment patterns of Figures 5 and 6. The positive correlation between La/Lu and La/Nd shows simultaneous MREE and HREE enrichment. Low Th/U is indicative of an increasing input of organic-rich sediments in the marine setting (Abanda and Hannigan, 2006). Because uranium is highly soluble in seawater, it will remain dissolved in seawater unless there are particles on which it can adsorb (Abanda and Hannigan, 2006). Organic matter also adsorbs onto the surface of similar particles that remove uranium from seawater (Abanda and Hannigan, 2006). As a result, there is typically a strong correlation between organic matter and the occurrence of uranium. In essence, both components (uranium and organic matter) are transported to the seafloor on the same grains. Thorium, inversely, is very insoluble and thus in a marine depositional setting Uranium enrichment is an indicator of organic content. Although there is notable scatter in the data, specifically in those samples that approach detection limits, we observe a general positive trend in Th/U vs. La/Nd in Figure 8, which reveals a general trend of uranium enrichment and MREE enrichment (Arthur and Sageman, 1994; Sageman et al., 2003; Straeten et al., 2011; Vine and Tourtelot, 1970; Wignall, 1991; Wignall and Newton, 2001).

Together, the results show strong indicators of coupled high primary productivity, likely associated with phosphate as a key limiting nutrient, adsorption of organic matter and uranium, followed by subsequent water-rock interactions of plagioclase and phosphate weathering with increasing geothermal gradients after burial (Figures 5-8). When viewed together, these factors are consistent with what we know about the high primary productivity, shallow marine black shale depositional setting of black shales from the Marcellus Group. We are able to use these figures in order to identify post-depositional weathering of black shales and thus verify the viability of the dilution method by using the results of the dilution method to confirm expected associated REE enrichment trends.

CONCLUSIONS

1) The broad suite of elemental analytes combined with the contrast of analytes at extremely high and low concentrations in flowback fluid causes interferences (such as the high barium oxide signal interfering with trace Eu).
2) Perform analysis on separate suites of elements, particularly in groups of similar expected concentration, would likely reduce interference.
3) Other analytical methods such as isotope dilution may be used to reduce the effect of spectral overlap as a result of analyzing trace and extremely high concentration elements simultaneously.
4) Dilution by a factor of 200 proved to be an effective method for reducing saline matrix of flowback and analyzing their REE concentrations.
5) Samples show high Ca and Ba concentrations, as well as patterns of "high hat" and HREE enrichment. The concentrations of Ca and Ba indicate that Marcellus black shales are dominated by plagioclase feldspar and phosphate weathering.

RECOMMENDATIONS FOR FUTURE WORK

Despite the failure of the chelating resin by this method, there is still potential for significant improvement of flowback analytical capabilities by pre-concentration of trace elements and reduction of saline matrix. Since the analytes were dissolved into solution, but not present by the time of analysis by ICP-MS there are only two potential steps in which the analytes were washed out of solution. First, the analytes may not have bound to the chelating resin and thus poured off in the supernatant liquid. To determine whether this is the case, one should repeat the current analytical method and, instead of disposing of the supernatant, retain and analyze it by ICP-MS. If the trace elements are present in this analysis, then it can be determined that they never bound to the resin and thus the pH of the solution needs to be investigated. Conversely, if the trace elements are not detected in the supernatant, then the analytes must be bound to the resin or other particle surfaces in the high TDS fluids and are not being released during re-acidification perhaps because of the high cation exchange capacity (buffering capacity) of the high TDS solutions. In this case, further work would involve validating re-acidification in the final stage of the original method.

In addition to diagnosis and resolution of the problems with the SPR-IDA method, additional work can be done to refine the dilution methods. Primarily, detection limits for elements typically above or below detection limits may be improved by performing separate analyses for suites of elements with similar expected concentrations. Ca, Al, Ba and other extremely concentrated elements may be analyzed using a 500x dilution factor or trace elements may be brought more comfortably above quantitation limits by using a 150x dilution for these analytes.

Further methods and instrumentation may also be utilized. These could include pre-screening flowback samples by ICP-OES or IC to avoid high Ca, Ba, Al or optimizing dilution factors, while reducing costs compared to ICP-MS analysis. Further, standard addition or isotope dilution may be integrated into the current dilution methodology. Finally, although this would present its own analytical challenges, the adaptations of a truly matrix matched analysis could help improve calibration, method development, and quantitative results.

REFERENCES CITED

Abanda, P.A. and Hannigan, R.E. (2006) Effect of diagenesis on trace element partitioning in shales. Chemical Geology 230, 42-59.

Arthur, M.A. and Sageman, B.B. (1994) Marine sahles: depositional mechanisms and environments of ancient deposits. Annual Review of Earth and Planetary Sciences 22, 499-551.

Bofinger, V.M. and Compston, W. (1967) A reassessment of age of Hamilton Group in New York and Pennsylvania and the role of inherited radiogneic Sr-87. Geochimica Et Cosmochimica Acta 31, 2353-2357.

Brantley, S.L., Yoxtheimer, D., Arjmand, S., Grieve, P., Vidic, R., Pollak, J., Llewellyn, G.T., Abad, J. and Simon, C. (2014) Water resource impacts during unconvetional shale gas development: The Pennsylvania experience. International Journal of Coal Geology 126, 140-156.

Briskin, J. (2015) Potential impacts of hydraulic fracturing for oil and gas on drinking water resources. Groundwater 53, 19-21.

Cuoco, E., Tedesco, D., Poreda, R.J., Williams, J.C., De Francesco, S., Balagizi, C. and Darrah, T.H. (2013) Impact of volcanic plume emissions on rain water chemistry during the January 2010 Nyamuragira eruptive event: Implications for essential potable water resources. Journal of Hazardous Materials 244, 570-581.

Darrah, T.H., Jackson, R.B., Vengosh, A., Warner, N.R. and Poreda, R.J. (2015a) Noble Gases: A New Technique for Fugitive Gas Investigation in Groundwater. Groundwater 53, 23-28.

Darrah, T.H., Jackson, R.B., Vengosh, A., Warner, N.R., Whyte, C.J., Walsh, T.B., Kondash, A.J. and Poreda, R.J. (2015b) The evolution of Devonian hydrocarbon gases in shallow aquifers of the northern Appalachian Basin: Insights from integrating noble gas and hydrocarbon geochemistry. Geochimica Et Cosmochimica Acta 170, 321-355.

Darrah, T.H., Prutsman-Pfeiffer, J.J., Poreda, R.J., Campbell, M.E., Hauschka, P.V. and Hannigan, R.E. (2009) Incorporation of excess gadolinium into human bone from medical contrast agents. Metallomics 1, 479-488.

Darrah, T.H., Vengosh, A., Jackson, R.B., Warner, N.R. and Poreda, R.J. (2014) Noble gases identify the mechanisms of fugitive gas contamination in drinking-water wells overlying the Marcellus and Barnett Shales. Proceedings of the National Academy of Sciences of the United States of America 111, 14076-14081.

Drollette, B.D., Hoelzer, K., Warner, N.R., Darrah, T.H., Karatum, O., O'Connor, M.P., Nelson, R.K., Fernandez, L.A., Reddy, C.M., Vengosh, A., Jackson, R.B., Elsner, M. and Plata, D.L. (2015) Elevated levels of diesel range organic compounds in groundwater near Marcellus gas operations are derived from surface activities. Proceedings of the National Academy of Sciences of the United States of America 112, 13184-13189.

Ellsworth, W.L. (2013) Injection-Induced Earthquakes. Science 341, 142-+.

Evans, M.A. (1994) Joints and decollement zonse in Middle Devonian shales- evidence for multiple deformation events in the central Appalachian Plateau Geological Society of America Bulletin 106, 447-460.

Evans, M.A. (1995) Fluid inclusions in veins from the Middle Devonian shales: a record of deformation conditions and fluid evolution in the Appalachian Plateau. Geological Society of America Bulletin 107.

Evans, M.A. and Battles, D.A. (1999) Fluid inclusion and stable isotope analyses of veins from the central Appalachian Valley and Ridge province: Implications for regional synorogenic hydrologic structure and fluid migration. Geological Society of America Bulletin 111, 1841-1860.
Faill, R.T. (1997a) A geological history of hte north-central Appalachians 1. Orogenesis from the mesoproterozoic through the taconic orogeny. American Journal of Science 297, 551-619.
Faill, R.T. (1997b) A geological history of the north-central Appalachians 2. Orogenesis from the Silurian through the Carboniferous. American Journal of Science 291, 729-761.
Faill, R.T. (2011) Folds of Pennsylvania-GIS data and map, in: Survey, P.G. (Ed.).
Haluszczak, L.O., Rose, A.W. and Kump, L.R. (2013) Geochemical evaluation of flowback brine from Marcellus gas wells in Pennsylvania, USA. Applied Geochemistry 28, 55-61.
Hannigan, R.E. and Sholkovitz, E.R. (2001) The development of middle rare earth element enrichments in freshwaters: weathering of phosphate minerals. Chemical Geology 175, 495-508.
Harkness, J.S., Dwyer, G.S., Warner, N.R., Parker, K.M., Mitch, W.A. and Vengosh, A. (2015) Iodide, Bromide, and Ammonium in Hydraulic Fracturing and Oil and Gas Wastewaters: Environmental Implications. Environmental Science & Technology 49, 1955-1963.
Howarth, R.W., Ingraffea, A. and Engelder, T. (2011) Natural gas: Should fracking stop? Nature 477, 271-275.
Jackson, R.B., Vengosh, A., Carey, J.W., Davies, R.J., Darrah, T.H., O'Sullivan, F. and Petron, G. (2014) The environmental costs and benefits of fracking. Annual Review of Environment and Resources 39.
Jerez, V. S. F., Godoy, J. M., de, C. R. C., & Gonc□alves, R. A. (January 01, 2013). Trace element determination in seawater by ICP-MS using online, offline and bath procedures of preconcentration and matrix elimination. *Microchemical Journal, 106,* 121-128.
Kerr, R.A. (2010) Natural Gas From Shale Bursts Onto the Scene. Science 328, 1624-1626.
Kondash, A. and Vengosh, A. (2015) Water Footprint of Hydraulic Fracturing. Environmental Science & Technology Letters 2, 276-280.
Lash, G.G. and Engelder, T. (2009) Tracking the burial and tectonic history of Devonian shale of the Appalachian Basin by analysis of joint intersection style. Geological Society of America Bulletin 121, 265-277.
Lash, G.G. and Engelder, T. (2011) Thickness trends and sequence stratigraphy of the Middle Devonian Marcellus Formation, Appalachian Basin: Implications for Acadian foreland basin evolution. Aapg Bulletin 95, 61-103.
Osborn, S.G. and McIntosh, J.C. (2010) Chemical and isotopic tracers of the contribution of microbial gas in Devonian organic-rich shales and reservoir sandstones, northern Appalachian Basin. Applied Geochemistry 25, 456-471.
Osborn, S.G., McIntosh, J.C., Hanor, J.S. and Biddulph, D. (2012) Iodine-129, Sr-87/Sr-86, and trace elemental geochemistry of northern Appalachian Basin brines:: evidence for basinal-scale fluid migration and clay mineral diagenesis. American Journal of Science 312, 263-287.
Parker, K.M., Zeng, T., Harkness, J., Vengosh, A. and Mitch, W.A. (2014) Enhanced Formation of Disinfection Byproducts in Shale Gas Wastewater-Impacted Drinking Water Supplies. Environmental Science & Technology 48, 11161-11169.
Peucker-Ehrenbrink, B. and Hannigan, R.E. (2000) Effects of black shale weathering on the mobility of rhenium and platinum group elements. Geology 28, 475-478.

Rahm, B.G., Bates, J.T., Bertoia, L.R., Galford, A.E., Yoxtheimer, D.A. and Riha, S.J. (2013) Wastewater management and Marcellus Shale gas development: Trends, drivers, and planning implications. Journal of Environmental Management 120, 105-113.
Ryder, R.T., Aggen, K.L., Hettinger, R.D., Law, B.E., Miller, J.J., Nuccio, V.F., Perry, W.J., Prensky, S.E., SanFilipo, J.R. and Wandry, C.J. (1996) Possible continous-type (unconventional) gas accumulation in the Lower Silurian "Clinton" sands, Medina Group, and Tuscarora Sandstone in teh Appalachian Basin: A progress report of 1995 activities, in: Survey, U.S.G. (Ed.). USGS, Washington, D.C.
Sageman, B.B., Murphy, A.E., Werne, J.P., Straeten, C.A.V., Hollander, D.J. and Lyons, T.W. (2003) A tale of shales: the relative roles of production, decomposition, and dilution in the accumulation of organic-rich strata, Middle-Upper Devonian, Appalachian Basin. Chemical Geology 195, 229-273.
Sak, P.B., McQuarrie, N., Oliver, B.P., Lavdovsky, N. and Jackson, M.S. (2012) Unraveling the central Appalachian fold-thrust belt, Pennsylvania: the power of sequentially restored balanced cross sections for a blind fold-thurst belt. Geosphere 8, 685-702.
Scanlin, M.A. and Engelder, T. (2003) The basement versus the no basement hypotheses for folding within the Appalachian plateau detachment sheet. American Journal of Science 303, 519-563.
Straeten, C.A.V., Brett, C.E. and Sageman, B.B. (2011) Mudrock sequence stratigraphy: a multi-proxy (sedimentoogical, paleobiological, and geochemical) approach, Devonian Appalachian Basin. Palaeogeography Palaeoclimatology Palaeoecology 304, 54-73.
Taylor, S.R. and McLennan, S.M. (1995) The geochemical evolution of the continental crust. Reviews of Geophysics 33, 241-265.
Thomas, R. (2003) Practical Guide to ICP-MS. Taylor and Francis, London, UK.
USGS (2011) National Field Manual for the collection of water-quality data, US Geological Survey, Washington, DC.
Vengosh, A., Jackson, R.B., Warner, N., Darrah, T.H., Kondash, A., (2014) A critical review of the risks to water resources from unconventional shale gas development and hydraulic fracturing in the United States. Environmental Science & Technology 48, 8334-8348.
Vengosh, A., Warner, N., Jackson, R. and Darrah, T. (2013) The effects of shale gas exploration and hydraulic fracturing on the quality of water resources in the United States, in: Hellmann, R., Pitsch, H. (Eds.), Proceedings of the Fourteenth International Symposium on Water-Rock Interaction, Wri 14, pp. 863-866.
Vidic, R.D., Brantley, S.L., Vandenbossche, J.M., Yoxtheimer, D. and Abad, J.D. (2013) Impact of Shale Gas Development on Regional Water Quality. Science 340.
Vine, J.D. and Tourtelot, E.B. (1970) Geochemistry of black shale deposits: a summary report. Economic Geology 65, 253-272.
Warner, N.R., Christie, C.A., Jackson, R.B. and Vengosh, A. (2013) Impacts of Shale Gas Wastewater Disposal on Water Quality in Western Pennsylvania. Environmental Science & Technology 47, 11849-11857.
Warner, N.R., Darrah, T.H., Jackson, R.B., Millot, R., Kloppman, W. and Vengosh, A. (2014) New tracers identify hydraulic fracturing fluids and accidental releases from oil and gas operations. environmental Science & Technology dx.doi.org/10.1021/es5032135.
Warner, N.R., Jackson, R.B., Darrah, T.H., Osborn, S.G., Down, A., Zhao, K.G., White, A. and Vengosh, A. (2012) Geochemical evidence for possible natural migration of Marcellus

Formation brine to shallow aquifers in Pennsylvania. Proceedings of the National Academy of Sciences of the United States of America 109, 11961-11966.
Wignall, P.B. (1991) Model for transgressive black shales. Geology 19, 167-170.
Wignall, P.B. and Newton, R. (2001) Black shales on the basin margin: a model based on examples from the Upper Jurassic of the Boulonnais, northern France. Sedimentary Geology 144, 335-356.

APPENDIX

Appendix 1. Analyte correlation matrix. Note that significant correlations ($p<0.05$) were highlighted in green.

		B11	Al27	Ca43	Sc45	Ti48	V51	Cr52	Fe54	Mn55
B11(MR)	Pearson Correlation	1	-.028	-.127	.138	.104	-.164	-.088	-.044	-.071
	Sig. (2-tailed)		.844	.376	.333	.469	.250	.539	.757	.622
	N	51	51	51	51	51	51	51	51	51
		Ni58	Co59	Cu65	Zn66	As75	Se82	Ag109	Cd111	Cs133
B11(MR)	Pearson Correlation	-.038	-.082	-.031	.241	-.064	.294*	.803**	.851**	.895**
	Sig. (2-tailed)	.793	.569	.827	.088	.654	.036	.000	.000	.000
	N	51	51	51	51	51	51	51	51	51
		Ba135	La139	Ce140	Pr141	Nd143	Sm147	Eu153	Gd157	Tb159
B11(MR)	Pearson Correlation	.574**	.554**	.031	.058	.338*	.668**	.676**	.678**	.441**
	Sig. (2-tailed)	.000	.000	.830	.687	.015	.000	.000	.000	.001
	N	51	51	51	51	51	51	51	51	51
		Dy161	Ho165	Er166	Tm169	Yb172	Lu175	Pb208	Th232	U238
B11(MR)	Pearson Correlation	.721**	.762**	.317*	.752**	.750**	.536**	.582**	.448**	.360**
	Sig. (2-tailed)	.000	.000	.023	.000	.000	.000	.000	.001	.010
	N	51	51	51	51	51	51	51	51	51
		B11	Al27	Ca43	Sc45	Ti48	V51	Cr52	Fe54	Mn55
Al27(MR)	Pearson Correlation		1	.102	.154	.206	.280*	.149	.259	.326*
	Sig. (2-tailed)			.477	.281	.147	.047	.296	.067	.020
	N		51	51	51	51	51	51	51	51
		Ni58	Co59	Cu65	Zn66	As75	Se82	Ag109	Cd111	Cs133
Al27(MR)	Pearson Correlation	.311*	.654**	.621**	.200	-.046	-.055	-.024	-.043	-.045
	Sig. (2-tailed)	.026	.000	.000	.159	.748	.699	.868	.762	.753
	N	51	51	51	51	51	51	51	51	51
		Ba135	La139	Ce140	Pr141	Nd143	Sm147	Eu153	Gd157	Tb159
Al27(MR)	Pearson Correlation	-.011	.009	-.003	-.018	-.029	-.032	-.032	-.030	-.050
	Sig. (2-tailed)	.939	.952	.982	.901	.840	.826	.826	.835	.728
	N	51	51	51	51	51	51	51	51	51
		Dy161	Ho165	Er166	Tm169	Yb172	Lu175	Pb208	Th232	U238
Al27(MR)	Pearson Correlation	-.023	-.011	.003	-.022	-.019	-.038	.070	.332*	.325*
	Sig. (2-tailed)	.874	.936	.982	.876	.893	.792	.628	.017	.020
	N	51	51	51	51	51	51	51	51	51
		B11	Al27	Ca43	Sc45	Ti48	V51	Cr52	Fe54	Mn55
Ca43(MR)	Pearson Correlation			1	-.164	.038	.143	-.084	-.061	.005
	Sig. (2-tailed)				.249	.791	.317	.558	.668	.974
	N			51	51	51	51	51	51	51
		Ni58	Co59	Cu65	Zn66	As75	Se82	Ag109	Cd111	Cs133
Ca43(MR)	Pearson Correlation	-.052	.243	.359**	.010	-.035	-.127	-.104	-.120	-.112
	Sig. (2-tailed)	.718	.085	.010	.946	.809	.374	.469	.402	.436
	N	51	51	51	51	51	51	51	51	51
		Ba135	La139	Ce140	Pr141	Nd143	Sm147	Eu153	Gd157	Tb159
Ca43(MR)	Pearson Correlation	-.117	-.133	-.054	-.058	-.091	-.137	-.128	-.140	.027
	Sig. (2-tailed)	.416	.351	.704	.686	.524	.337	.371	.327	.850
	N	51	51	51	51	51	51	51	51	51
		Dy161	Ho165	Er166	Tm169	Yb172	Lu175	Pb208	Th232	U238
Ca43(MR)	Pearson Correlation	-.125	-.120	-.081	-.135	-.145	-.113	-.016	-.028	-.099
	Sig. (2-tailed)	.384	.403	.570	.343	.310	.431	.909	.846	.490
	N	51	51	51	51	51	51	51	51	51

Appendix 1 (Continued). Analyte correlation matrix.

		B11	Al27	Ca43	Sc45	Ti48	V51	Cr52	Fe54	Mn55
Sc45(MR)	Pearson Correlation				1	.904**	-.006	.166	.252	.773**
	Sig. (2-tailed)					.000	.969	.246	.075	.000
	N				51	51	51	51	51	51
		Ni58	Co59	Cu65	Zn66	As75	Se82	Ag109	Cd111	Cs133
Sc45(MR)	Pearson Correlation	.268	.262	.130	.426**	-.155	.501**	.119	.118	.199
	Sig. (2-tailed)	.057	.063	.362	.002	.278	.000	.406	.410	.162
	N	51	51	51	51	51	51	51	51	51
		Ba135	La139	Ce140	Pr141	Nd143	Sm147	Eu153	Gd157	Tb159
Sc45(MR)	Pearson Correlation	.181	.211	.058	.063	.081	.232	.240	.171	.003
	Sig. (2-tailed)	.205	.136	.685	.660	.573	.101	.089	.231	.982
	N	51	51	51	51	51	51	51	51	51
		Dy161	Ho165	Er166	Tm169	Yb172	Lu175	Pb208	Th232	U238
Sc45(MR)	Pearson Correlation	.130	.142	.107	.305*	.439**	.104	.210	-.031	-.035
	Sig. (2-tailed)	.363	.319	.456	.030	.001	.469	.139	.830	.808
	N	51	51	51	51	51	51	51	51	51
		B11	Al27	Ca43	Sc45	Ti48	V51	Cr52	Fe54	Mn55
Ti48(MR)	Pearson Correlation					1	-.073	.160	.263	.874**
	Sig. (2-tailed)						.610	.263	.062	.000
	N					51	51	51	51	51
		Ni58	Co59	Cu65	Zn66	As75	Se82	Ag109	Cd111	Cs133
Ti48(MR)	Pearson Correlation	.284*	.352*	.288*	.415**	-.149	.433**	.063	.068	.155
	Sig. (2-tailed)	.044	.011	.041	.002	.297	.001	.658	.635	.278
	N	51	51	51	51	51	51	51	51	51
		Ba135	La139	Ce140	Pr141	Nd143	Sm147	Eu153	Gd157	Tb159
Ti48(MR)	Pearson Correlation	.125	.135	.004	.012	.016	.169	.192	.116	-.030
	Sig. (2-tailed)	.380	.344	.977	.934	.910	.236	.177	.419	.833
	N	51	51	51	51	51	51	51	51	51
		Dy161	Ho165	Er166	Tm169	Yb172	Lu175	Pb208	Th232	U238
Ti48(MR)	Pearson Correlation	.059	.069	.050	.244	.381**	.049	.175	-.144	-.163
	Sig. (2-tailed)	.682	.629	.729	.085	.006	.731	.219	.312	.252
	N	51	51	51	51	51	51	51	51	51
		B11	Al27	Ca43	Sc45	Ti48	V51	Cr52	Fe54	Mn55
V51(MR)	Pearson Correlation						1	.072	-.250	-.086
	Sig. (2-tailed)							.615	.076	.551
	N						51	51	51	51
		Ni58	Co59	Cu65	Zn66	As75	Se82	Ag109	Cd111	Cs133
V51(MR)	Pearson Correlation	-.247	-.010	-.071	-.090	-.135	-.290*	-.166	-.176	-.111
	Sig. (2-tailed)	.080	.944	.621	.532	.345	.039	.245	.218	.439
	N	51	51	51	51	51	51	51	51	51
		Ba135	La139	Ce140	Pr141	Nd143	Sm147	Eu153	Gd157	Tb159
V51(MR)	Pearson Correlation	-.042	-.151	-.118	-.147	-.199	-.208	-.182	-.191	-.170
	Sig. (2-tailed)	.771	.292	.408	.303	.161	.144	.201	.180	.232
	N	51	51	51	51	51	51	51	51	51
		Dy161	Ho165	Er166	Tm169	Yb172	Lu175	Pb208	Th232	U238
V51(MR)	Pearson Correlation	-.194	-.204	-.196	-.184	-.168	-.192	-.141	.366**	.372**
	Sig. (2-tailed)	.172	.152	.169	.197	.239	.176	.325	.008	.007
	N	51	51	51	51	51	51	51	51	51

		B11	Al27	Ca43	Sc45	Ti48	V51	Cr52	Fe54	Mn55
Cr52(MR)	Pearson Correlation							1	.112	.144
	Sig. (2-tailed)								.435	.314
	N							51	51	51
		Ni58	Co59	Cu65	Zn66	As75	Se82	Ag109	Cd111	Cs133
Cr52(MR)	Pearson Correlation	.132	.318*	.133	.165	-.027	.177	-.110	-.114	-.098
	Sig. (2-tailed)	.354	.023	.353	.246	.853	.214	.442	.424	.496
	N	51	51	51	51	51	51	51	51	51
		Ba135	La139	Ce140	Pr141	Nd143	Sm147	Eu153	Gd157	Tb159
Cr52(MR)	Pearson Correlation	-.006	-.099	-.050	-.052	-.088	-.096	-.088	-.104	-.120
	Sig. (2-tailed)	.969	.490	.729	.715	.537	.503	.541	.469	.403
	N	51	51	51	51	51	51	51	51	51
		Dy161	Ho165	Er166	Tm169	Yb172	Lu175	Pb208	Th232	U238
Cr52(MR)	Pearson Correlation	-.117	-.121	-.084	-.105	-.077	-.105	-.058	-.092	-.048
	Sig. (2-tailed)	.413	.398	.556	.464	.591	.465	.684	.519	.738
	N	51	51	51	51	51	51	51	51	51
		B11	Al27	Ca43	Sc45	Ti48	V51	Cr52	Fe54	Mn55
Fe54(MR)	Pearson Correlation								1	.284*
	Sig. (2-tailed)									.043
	N								51	51
		Ni58	Co59	Cu65	Zn66	As75	Se82	Ag109	Cd111	Cs133
Fe54(MR)	Pearson Correlation	.997**	.327*	.311*	.078	.077	.129	-.075	-.082	-.059
	Sig. (2-tailed)	.000	.019	.026	.587	.590	.366	.602	.567	.679
	N	51	51	51	51	51	51	51	51	51
		Ba135	La139	Ce140	Pr141	Nd143	Sm147	Eu153	Gd157	Tb159
Fe54(MR)	Pearson Correlation	-.050	.411**	.784**	.783**	.688**	.140	-.074	-.002	.139
	Sig. (2-tailed)	.728	.003	.000	.000	.000	.328	.607	.986	.331
	N	51	51	51	51	51	51	51	51	51
		Dy161	Ho165	Er166	Tm169	Yb172	Lu175	Pb208	Th232	U238
Fe54(MR)	Pearson Correlation	.071	.291*	.704**	.041	.007	-.069	.012	-.039	-.113
	Sig. (2-tailed)	.620	.038	.000	.773	.959	.632	.934	.787	.429
	N	51	51	51	51	51	51	51	51	51
		B11	Al27	Ca43	Sc45	Ti48	V51	Cr52	Fe54	Mn55
Mn55(MR)	Pearson Correlation									1
	Sig. (2-tailed)									
	N									51
		Ni58	Co59	Cu65	Zn66	As75	Se82	Ag109	Cd111	Cs133
Mn55(MR)	Pearson Correlation	.304*	.380**	.334*	.306*	-.097	.433**	-.029	-.033	-.029
	Sig. (2-tailed)	.030	.006	.017	.029	.496	.002	.840	.818	.843
	N	51	51	51	51	51	51	51	51	51
		Ba135	La139	Ce140	Pr141	Nd143	Sm147	Eu153	Gd157	Tb159
Mn55(MR)	Pearson Correlation	-.073	.072	-.049	-.044	-.063	.117	.164	.064	-.054
	Sig. (2-tailed)	.610	.615	.730	.761	.663	.415	.251	.657	.706
	N	51	51	51	51	51	51	51	51	51
		Dy161	Ho165	Er166	Tm169	Yb172	Lu175	Pb208	Th232	U238
Mn55(MR)	Pearson Correlation	-.035	-.045	-.020	.164	.315*	.043	.100	-.122	-.120
	Sig. (2-tailed)	.808	.756	.889	.249	.024	.766	.484	.394	.400
	N	51	51	51	51	51	51	51	51	51

Appendix 1 (continued). Analyte correlation matrix

Appendix 1 (continued). Analyte correlation matrix

		Ni58	Co59	Cu65	Zn66	As75	Se82	Ag109	Cd111	Cs133
Ni58(MR)	Pearson Correlation	1	.374**	.360**	.108	.053	.119	-.069	-.079	-.052
	Sig. (2-tailed)		.007	.009	.449	.714	.406	.628	.582	.718
	N	51	51	51	51	51	51	51	51	51
		Ba135	La139	Ce140	Pr141	Nd143	Sm147	Eu153	Gd157	Tb159
Ni58(MR)	Pearson Correlation	-.033	.392**	.750**	.749**	.658**	.133	-.073	-.004	.135
	Sig. (2-tailed)	.817	.004	.000	.000	.000	.354	.612	.980	.346
	N	51	51	51	51	51	51	51	51	51
		Dy161	Ho165	Er166	Tm169	Yb172	Lu175	Pb208	Th232	U238
Ni58(MR)	Pearson Correlation	.070	.281*	.675**	.040	.008	-.068	.020	-.038	-.111
	Sig. (2-tailed)	.627	.045	.000	.778	.958	.635	.892	.792	.439
	N	51	51	51	51	51	51	51	51	51
		Ni58	Co59	Cu65	Zn66	As75	Se82	Ag109	Cd111	Cs133
Co59(MR)	Pearson Correlation		1	.765**	.432**	-.084	.075	-.033	-.052	-.042
	Sig. (2-tailed)			.000	.002	.557	.602	.816	.717	.772
	N		51	51	51	51	51	51	51	51
		Ba135	La139	Ce140	Pr141	Nd143	Sm147	Eu153	Gd157	Tb159
Co59(MR)	Pearson Correlation	-.058	-.015	-.010	-.016	-.034	-.023	-.020	-.020	.073
	Sig. (2-tailed)	.688	.916	.947	.914	.810	.872	.891	.888	.611
	N	51	51	51	51	51	51	51	51	51
		Dy161	Ho165	Er166	Tm169	Yb172	Lu175	Pb208	Th232	U238
Co59(MR)	Pearson Correlation	-.009	-.023	-.012	-.001	.009	-.016	.159	.074	.105
	Sig. (2-tailed)	.948	.870	.931	.993	.949	.910	.266	.606	.462
	N	51	51	51	51	51	51	51	51	51
		Ni58	Co59	Cu65	Zn66	As75	Se82	Ag109	Cd111	Cs133
Cu65(MR)	Pearson Correlation			1	.308*	-.058	-.021	.015	-.008	.001
	Sig. (2-tailed)				.028	.687	.884	.917	.953	.994
	N			51	51	51	51	51	51	51
		Ba135	La139	Ce140	Pr141	Nd143	Sm147	Eu153	Gd157	Tb159
Cu65(MR)	Pearson Correlation	-.037	-.013	-.022	-.020	-.021	.003	.011	.026	.131
	Sig. (2-tailed)	.799	.929	.879	.887	.883	.984	.942	.858	.359
	N	51	51	51	51	51	51	51	51	51
		Dy161	Ho165	Er166	Tm169	Yb172	Lu175	Pb208	Th232	U238
Cu65(MR)	Pearson Correlation	.041	.006	.004	.035	.027	.008	.233	-.001	-.024
	Sig. (2-tailed)	.777	.969	.977	.809	.852	.953	.100	.997	.865
	N	51	51	51	51	51	51	51	51	51
		Ni58	Co59	Cu65	Zn66	As75	Se82	Ag109	Cd111	Cs133
Zn66(MR)	Pearson Correlation				1	-.107	.112	.255	.235	.280*
	Sig. (2-tailed)					.456	.433	.071	.096	.047
	N				51	51	51	51	51	51
		Ba135	La139	Ce140	Pr141	Nd143	Sm147	Eu153	Gd157	Tb159
Zn66(MR)	Pearson Correlation	.194	.105	-.086	-.075	.017	.198	.222	.285*	.142
	Sig. (2-tailed)	.174	.465	.550	.599	.907	.164	.118	.042	.320
	N	51	51	51	51	51	51	51	51	51
		Dy161	Ho165	Er166	Tm169	Yb172	Lu175	Pb208	Th232	U238
Zn66(MR)	Pearson Correlation	.367**	.188	.051	.331*	.313*	.186	.526**	.126	.090
	Sig. (2-tailed)	.008	.186	.724	.018	.025	.191	.000	.380	.530
	N	51	51	51	51	51	51	51	51	51

Appendix 1 (continued). Analyte correlation matrix

		Ni58	Co59	Cu65	Zn66	As75	Se82	Ag109	Cd111	Cs133
As75(HR)	Pearson Correlation					1	-.072	-.078	-.075	-.081
	Sig. (2-tailed)						.614	.587	.600	.570
	N					51	51	51	51	51
		Ba135	La139	Ce140	Pr141	Nd143	Sm147	Eu153	Gd157	Tb159
As75(HR)	Pearson Correlation	-.059	-.091	-.034	-.036	-.057	-.091	-.088	-.075	-.079
	Sig. (2-tailed)	.680	.527	.810	.801	.692	.525	.540	.603	.583
	N	51	51	51	51	51	51	51	51	51
		Dy161	Ho165	Er166	Tm169	Yb172	Lu175	Pb208	Th232	U238
As75(HR)	Pearson Correlation	-.070	-.076	-.059	-.092	-.100	-.067	-.068	-.086	-.042
	Sig. (2-tailed)	.626	.594	.680	.521	.483	.642	.635	.549	.771
	N	51	51	51	51	51	51	51	51	51
		Ni58	Co59	Cu65	Zn66	As75	Se82	Ag109	Cd111	Cs133
Se82(HR)	Pearson Correlation						1	.196	.248	.225
	Sig. (2-tailed)							.167	.079	.113
	N						51	51	51	51
		Ba135	La139	Ce140	Pr141	Nd143	Sm147	Eu153	Gd157	Tb159
Se82(HR)	Pearson Correlation	.071	.217	.057	.072	.148	.269	.286*	.189	.058
	Sig. (2-tailed)	.620	.126	.689	.617	.300	.056	.042	.184	.685
	N	51	51	51	51	51	51	51	51	51
		Dy161	Ho165	Er166	Tm169	Yb172	Lu175	Pb208	Th232	U238
Se82(HR)	Pearson Correlation	.150	.231	.143	.298*	.449**	.147	.190	.039	-.002
	Sig. (2-tailed)	.292	.104	.318	.034	.001	.305	.181	.783	.990
	N	51	51	51	51	51	51	51	51	51
		Ni58	Co59	Cu65	Zn66	As75	Se82	Ag109	Cd111	Cs133
Ag109(LR)	Pearson Correlation							1	.991**	.865**
	Sig. (2-tailed)								.000	.000
	N							51	51	51
		Ba135	La139	Ce140	Pr141	Nd143	Sm147	Eu153	Gd157	Tb159
Ag109(LR)	Pearson Correlation	.341*	.767**	.024	.057	.391**	.935**	.956**	.965**	.765**
	Sig. (2-tailed)	.014	.000	.869	.691	.005	.000	.000	.000	.000
	N	51	51	51	51	51	51	51	51	51
		Dy161	Ho165	Er166	Tm169	Yb172	Lu175	Pb208	Th232	U238
Ag109(LR)	Pearson Correlation	.930**	.865**	.379**	.944**	.871**	.905**	.730**	.680**	.635**
	Sig. (2-tailed)	.000	.000	.006	.000	.000	.000	.000	.000	.000
	N	51	51	51	51	51	51	51	51	51
		Ni58	Co59	Cu65	Zn66	As75	Se82	Ag109	Cd111	Cs133
Cd111(LR)	Pearson Correlation								1	.877**
	Sig. (2-tailed)									.000
	N								51	51
		Ba135	La139	Ce140	Pr141	Nd143	Sm147	Eu153	Gd157	Tb159
Cd111(LR)	Pearson Correlation	.382**	.754**	.027	.061	.397**	.919**	.942**	.937**	.735**
	Sig. (2-tailed)	.006	.000	.852	.672	.004	.000	.000	.000	.000
	N	51	51	51	51	51	51	51	51	51
		Dy161	Ho165	Er166	Tm169	Yb172	Lu175	Pb208	Th232	U238
Cd111(LR)	Pearson Correlation	.901**	.868**	.379**	.929**	.874**	.873**	.695**	.667**	.610**
	Sig. (2-tailed)	.000	.000	.006	.000	.000	.000	.000	.000	.000
	N	51	51	51	51	51	51	51	51	51

Appendix 1 (continued). Analyte correlation matrix

		Ni58	Co59	Cu65	Zn66	As75	Se82	Ag109	Cd111	Cs133
Cs133(LR)	Pearson Correlation									1
	Sig. (2-tailed)									
	N									51
		Ba135	La139	Ce140	Pr141	Nd143	Sm147	Eu153	Gd157	Tb159
Cs133(LR)	Pearson Correlation	.333*	.633**	.016	.041	.328*	.755**	.754**	.793**	.476**
	Sig. (2-tailed)	.017	.000	.909	.776	.019	.000	.000	.000	.000
	N	51	51	51	51	51	51	51	51	51
		Dy161	Ho165	Er166	Tm169	Yb172	Lu175	Pb208	Th232	U238
Cs133(LR)	Pearson Correlation	.850**	.836**	.328*	.880**	.874**	.600**	.762**	.446**	.401**
	Sig. (2-tailed)	.000	.000	.019	.000	.000	.000	.000	.001	.004
	N	51	51	51	51	51	51	51	51	51
		Ba135	La139	Ce140	Pr141	Nd143	Sm147	Eu153	Gd157	Tb159
Ba135(LR)	Pearson Correlation	1	.168	-.045	-.031	.091	.236	.262	.227	.296*
	Sig. (2-tailed)		.239	.752	.830	.523	.096	.064	.109	.035
	N	51	51	51	51	51	51	51	51	51
		Dy161	Ho165	Er166	Tm169	Yb172	Lu175	Pb208	Th232	U238
Ba135(LR)	Pearson Correlation	.202	.235	.056	.207	.169	.265	.015	.197	.160
	Sig. (2-tailed)	.155	.096	.699	.145	.236	.060	.914	.165	.263
	N	51	51	51	51	51	51	51	51	51
		Ba135	La139	Ce140	Pr141	Nd143	Sm147	Eu153	Gd157	Tb159
La139(LR)	Pearson Correlation		1	.620**	.643**	.845**	.921**	.782**	.824**	.780**
	Sig. (2-tailed)			.000	.000	.000	.000	.000	.000	.000
	N		51	51	51	51	51	51	51	51
		Dy161	Ho165	Er166	Tm169	Yb172	Lu175	Pb208	Th232	U238
La139(LR)	Pearson Correlation	.809**	.928**	.843**	.821**	.737**	.752**	.533**	.628**	.559**
	Sig. (2-tailed)	.000	.000	.000	.000	.000	.000	.000	.000	.000
	N	51	51	51	51	51	51	51	51	51
		Ba135	La139	Ce140	Pr141	Nd143	Sm147	Eu153	Gd157	Tb159
Ce140(LR)	Pearson Correlation			1	.999**	.926**	.281*	.012	.103	.275
	Sig. (2-tailed)				.000	.000	.046	.935	.471	.051
	N			51	51	51	51	51	51	51
		Dy161	Ho165	Er166	Tm169	Yb172	Lu175	Pb208	Th232	U238
Ce140(LR)	Pearson Correlation	.188	.473**	.929**	.132	.059	.027	.008	.129	.027
	Sig. (2-tailed)	.188	.000	.000	.354	.681	.848	.954	.369	.850
	N	51	51	51	51	51	51	51	51	51
		Ba135	La139	Ce140	Pr141	Nd143	Sm147	Eu153	Gd157	Tb159
Pr141(LR)	Pearson Correlation				1	.939**	.313*	.046	.136	.302*
	Sig. (2-tailed)					.000	.025	.749	.342	.031
	N				51	51	51	51	51	51
		Dy161	Ho165	Er166	Tm169	Yb172	Lu175	Pb208	Th232	U238
Pr141(LR)	Pearson Correlation	.217	.499**	.941**	.163	.088	.060	.030	.135	.030
	Sig. (2-tailed)	.127	.000	.000	.252	.538	.675	.834	.344	.837
	N	51	51	51	51	51	51	51	51	51

Appendix 1 (continued). Analyte correlation matrix

		Ba135	La139	Ce140	Pr141	Nd143	Sm147	Eu153	Gd157	Tb159
Nd143(LR)	Pearson Correlation					1	.600**	.363**	.446**	.529**
	Sig. (2-tailed)						.000	.009	.001	.000
	N					51	51	51	51	51
		Dy161	Ho165	Er166	Tm169	Yb172	Lu175	Pb208	Th232	U238
Nd143(LR)	Pearson Correlation	.511**	.754**	.996**	.465**	.374**	.356*	.271	.360**	.239
	Sig. (2-tailed)	.000	.000	.000	.001	.007	.010	.054	.009	.092
	N	51	51	51	51	51	51	51	51	51
		Ba135	La139	Ce140	Pr141	Nd143	Sm147	Eu153	Gd157	Tb159
Sm147(LR)	Pearson Correlation						1	.961**	.968**	.830**
	Sig. (2-tailed)							.000	.000	.000
	N						51	51	51	51
		Dy161	Ho165	Er166	Tm169	Yb172	Lu175	Pb208	Th232	U238
Sm147(LR)	Pearson Correlation	.910**	.910**	.595**	.947**	.876**	.921**	.664**	.668**	.620**
	Sig. (2-tailed)	.000	.000	.000	.000	.000	.000	.000	.000	.000
	N	51	51	51	51	51	51	51	51	51
		Ba135	La139	Ce140	Pr141	Nd143	Sm147	Eu153	Gd157	Tb159
Eu153(LR)	Pearson Correlation							1	.970**	.789**
	Sig. (2-tailed)								.000	.000
	N							51	51	51
		Dy161	Ho165	Er166	Tm169	Yb172	Lu175	Pb208	Th232	U238
Eu153(LR)	Pearson Correlation	.874**	.799**	.355*	.938**	.890**	.955**	.667**	.665**	.641**
	Sig. (2-tailed)	.000	.000	.011	.000	.000	.000	.000	.000	.000
	N	51	51	51	51	51	51	51	51	51
		Ba135	La139	Ce140	Pr141	Nd143	Sm147	Eu153	Gd157	Tb159
Gd157(LR)	Pearson Correlation								1	.793**
	Sig. (2-tailed)									.000
	N								51	51
		Dy161	Ho165	Er166	Tm169	Yb172	Lu175	Pb208	Th232	U238
Gd157(LR)	Pearson Correlation	.959**	.858**	.447**	.966**	.878**	.940**	.770**	.670**	.638**
	Sig. (2-tailed)	.000	.000	.001	.000	.000	.000	.000	.000	.000
	N	51	51	51	51	51	51	51	51	51
		Ba135	La139	Ce140	Pr141	Nd143	Sm147	Eu153	Gd157	Tb159
Tb159(LR)	Pearson Correlation									1
	Sig. (2-tailed)									
	N									51
		Dy161	Ho165	Er166	Tm169	Yb172	Lu175	Pb208	Th232	U238
Tb159(LR)	Pearson Correlation	.702**	.701**	.506**	.684**	.547**	.871**	.373**	.655**	.643**
	Sig. (2-tailed)	.000	.000	.000	.000	.000	.000	.007	.000	.000
	N	51	51	51	51	51	51	51	51	51
		Dy161	Ho165	Er166	Tm169	Yb172	Lu175	Pb208	Th232	U238
Dy161(LR)	Pearson Correlation	1	.901**	.521**	.959**	.861**	.827**	.869**	.621**	.565**
	Sig. (2-tailed)		.000	.000	.000	.000	.000	.000	.000	.000
	N	51	51	51	51	51	51	51	51	51
		Dy161	Ho165	Er166	Tm169	Yb172	Lu175	Pb208	Th232	U238
Ho165(LR)	Pearson Correlation		1	.750**	.895**	.828**	.716**	.683**	.588**	.500**
	Sig. (2-tailed)			.000	.000	.000	.000	.000	.000	.000
	N		51	51	51	51	51	51	51	51

Appendix 1 (continued). Analyte correlation matrix

		Dy161	Ho165	Er166	Tm169	Yb172	Lu175	Pb208	Th232	U238
Er166(LR)	Pearson Correlation			1	.474**	.384**	.341*	.305*	.345*	.224
	Sig. (2-tailed)				.000	.005	.014	.029	.013	.114
	N			51	51	51	51	51	51	51
		Dy161	Ho165	Er166	Tm169	Yb172	Lu175	Pb208	Th232	U238
Tm169(LR)	Pearson Correlation				1	.964**	.840**	.832**	.594**	.545**
	Sig. (2-tailed)					.000	.000	.000	.000	.000
	N				51	51	51	51	51	51
		Dy161	Ho165	Er166	Tm169	Yb172	Lu175	Pb208	Th232	U238
Yb172(LR)	Pearson Correlation					1	.731**	.789**	.491**	.444**
	Sig. (2-tailed)						.000	.000	.000	.001
	N					51	51	51	51	51
		Dy161	Ho165	Er166	Tm169	Yb172	Lu175	Pb208	Th232	U238
Lu175(LR)	Pearson Correlation						1	.566**	.704**	.700**
	Sig. (2-tailed)							.000	.000	.000
	N						51	51	51	51
		Dy161	Ho165	Er166	Tm169	Yb172	Lu175	Pb208	Th232	U238
Pb208(LR)	Pearson Correlation							1	.409**	.352*
	Sig. (2-tailed)								.003	.011
	N							51	51	51
		Dy161	Ho165	Er166	Tm169	Yb172	Lu175	Pb208	Th232	U238
Th232(LR)	Pearson Correlation								1	.964**
	Sig. (2-tailed)									.000
	N								51	51
		Dy161	Ho165	Er166	Tm169	Yb172	Lu175	Pb208	Th232	U238
U238(LR)	Pearson Correlation									1
	Sig. (2-tailed)									
	N									51

Table 2. Analyte concentrations corrected for dilution of samples PAG B3 – PAG B4 (ppt)

Element	Atomic Mass	PAG B3	NY C29	NY C13	NY C14	Marcellus D34	Marcellus D62	Flowback B	PAG B3	NY C18	Hark EFF	PAG B4
B	11	bdl	bdl	bdl	bdl	bdl	bdl	bdl	4	1	1	1
Al	27	4.22	3381.35	adl	adl	adl	adl	adl	223.60	456.99	adl	adl
Ca	43	adl	adl	adl	adl	adl	adl	adl	7.92E+06	3.73E+09	2.88E+09	5.83E+07
Sc	45	0.08	9.96	4.52	1.55	2.60	4.33	1.09	bdl	2.56	2.02	bdl
Ti	48	655	611524	241296	157697	183374	317503	92956	545	265560	232275	3997
V	51	0.22	1.68	3.76	1.48	9.94	1.44	1.23	bdl	0.54	0.48	0.01
Cr	52	25.98	74.30	816.18	43.13	115.77	36.97	809.76	15.41	161.51	80.05	22.08
Fe	54	349	607092	266222	30956	99840	358849	284	328	407536	133	4796
Mn	55	362	771251	89729	58637	53505	123111	10360	324	151728	419	1310
Ni	58	bdl	4603.27	2189.13	52.42	522.99	2587.87	bdl	10.62	3566.94	bdl	29.29
Co	59	bdl	27.73	31.68	6.06	bdl	5.06	9.71	bdl	98.69	1.67	0.36
Cu	65	34.34	1381.79	281.89	7.32	185.04	79.79	114.24	bdl	300.99	bdl	11.95
Zn	66	364	1511	3971	1214	2566	6222	290	310	5757	2433	572
As	75	bdl	70.48	504.49	146.63	107.72	bdl	4.33	bdl	43.57	87.01	46.65
Se	82	251	1765	889	698	635	551	664	167	195	557	325
Ag	109	bdl	1.33	0.57	0.68	0.42	5.21	1.02	bdl	1.06	0.40	0.14
Cd	111	bdl	82.21	68.29	53.28	27.38	259.72	36.33	bdl	32.23	26.21	5.29
Cs	133	0.16	937.62	204.01	331.68	255.90	3666.02	636.97	bdl	428.04	539.17	bdl
Ba	135	3596	bdl	143910	214343	43200	1421	bdl	4379	75009	8249	111836
La	139	0.55	416.99	4.81	4.53	1.60	142.44	176.17	0.04	4.51	0.18	1.68
Ce	140	bdl	58.24	2.64	0.30	0.22	10.34	8.60	bdl	6.78	bdl	bdl
Pr	141	0.01	9.76	0.33	0.15	bdl	2.11	1.85	bdl	0.44	bdl	bdl
Nd	143	0.05	43.65	10.42	9.19	7.79	46.72	12.41	0.78	10.11	11.54	4.25
Sm	147	bdl	169.69	1.97	2.46	0.44	66.63	77.20	0.07	1.83	0.53	0.38
Eu	153	1.6	12411	88	127	30.9	4028	5464	0.40	34	bdl	57
Gd	157	bdl	593.80	18.30	14.16	7.62	231.21	266.61	bdl	bdl	bdl	bdl
Tb	159	0.56	1.87	0.62	0.58	bdl	4.13	0.59	0.41	bdl	0.74	8.91
Dy	161	0.12	16.92	4.63	3.80	2.78	18.73	7.97	bdl	2.64	1.71	bdl
Ho	165	0.55	2.06	0.07	0.08	0.03	0.40	0.07	0.56	0.16	0.09	bdl
Er	166	bdl	6.67	bdl	bdl	bdl	1.66	0.43	bdl	0.00	bdl	bdl
Tm	169	bdl	10.06	0.14	0.13	0.01	4.29	2.22	0.01	0.23	0.11	0.01
Yb	172	12.91	179.64	1.27	1.31	0.01	43.88	22.72	14.53	0.89	0.01	bdl
Lu	175	0.19	69.07	2.19	1.54	0.43	21.62	10.88	bdl	0.79	0.82	6.52
Pb	208	26.07	866.53	854.43	11.28	73.33	642.25	14.19	20.17	1785.73	0.81	2.95
Th	232	bdl	bdl	bdl	bdl	bdl	bdl	bdl	0.09	0.14	0.06	0.20
U	238	bdl	0.06	0.14	0.08	0.01	0.71	1.24	bdl	0.38	0.13	1.10
La/Nd		11.72	9.55	0.46	0.49	0.21	3.05	14.20	0.05	0.45	0.02	0.39
La/Lu		2.95	6.04	2.19	2.93	3.72	6.59	16.20	bdl	5.73	0.22	0.26
Ba/Nd		7.7E+04	bdl	1.4E+04	2.3E+04	5.55E+03	3.04E+01	bdl	5.60E+03	7.42E+03	7.15E+02	2.63E+04
Th/U		bdl	bdl	bdl	bdl	bdl	bdl	bdl	bdl	0.37	0.45	0.18

Table 2 (continued). Analyte concentrations corrected for dilution of samples NY C16 – Marcellus D61(ppt)

Element	Atomic Mass	NY C16	NY C12	NY C23	ARK Davis	ARK Baker	Marcellus D6	NY Herkimer Comb	NY Site A	ARK Collums	Marcellus D61
B	11	3	1	4	1	1	1	1	17984	32635	634642
Al	27	4097.53	adl	adl	adl	adl	adl	163.68	80.71	adl	24.54
Ca	43	4.84E+09	1.06E+09	1.76E+09	4.49E+07	3.09E+07	2.21E+09	3.48E+09	3.48E+07	6.07E+04	4.83E+07
Sc	45	0.91	0.09	1.12	bdl	bdl	0.90	1.45	4.20	bdl	10.18
Ti	48	317942	77456	151943	3476	1475	161469	231852	232838	400	410661
V	51	0.44	0.19	0.76	bdl	1.33	0.27	2.64	bdl	bdl	bdl
Cr	52	68.22	90.87	62.83	16.31	608.79	105.95	139.16	207.06	25.21	155.79
Fe	54	202141	67	114	47254	76581	330287	584472	155517	184	399962
Mn	55	368981	3435	2044	48	818	31826	175079	100716	45	102084
Ni	58	1677.52	24.28	3.14	411.45	573.48	2600.19	4723.17	1231.47	58.64	3356.53
Co	59	87.94	2.08	2.12	bdl	4.80	0.67	113.95	17.11	1.60	1.90
Cu	65	3352.58	bdl	485.07	bdl	bdl	1027.64	4107.29	32.17	71.89	140.78
Zn	66	4065	660	1615	2767	1810	472	8565	1056	785	8142
As	75	90.56	472.08	2266.78	2.64	29.99	1493.61	bdl	14.00	8.56	11.80
Se	82	392	345	258	103	248	276	285	766	bdl	15741
Ag	109	2.71	0.55	0.78	0.14	0.12	0.14	1.06	1.15	bdl	19.63
Cd	111	66.94	27.07	29.32	12.51	10.78	12.96	35.47	72.57	23.68	892.30
Cs	133	340.25	140.05	257.81	bdl	bdl	152.64	504.22	349.92	13.24	8306.22
Ba	135	bdl	3348	7917	33118	24970	31094	66050	769226	2090	1682702
La	139	164.03	bdl	bdl	1.24	0.69	0.34	6.37	12.45	0.14	233.54
Ce	140	73.05	bdl	0.14	0.13	0.30	0.29	1.86	1.63	0.07	35.25
Pr	141	8.47	bdl	0.10	bdl	bdl	bdl	0.22	0.78	0.23	8.28
Nd	143	44.86	10.44	8.91	8.10	11.38	7.05	10.80	18.68	9.51	229.49
Sm	147	61.70	0.98	1.04	0.46	bdl	0.16	1.44	6.40	0.06	112.33
Eu	153	4699	3.0	bdl	11.5	7.6	8.4	22	365	bdl	7622
Gd	157	129.24	bdl	bdl	bdl	bdl	bdl	bdl	bdl	bdl	412.30
Tb	159	1.66	0.89	bdl	0.25	bdl	bdl	69.04	0.75	1.27	17.24
Dy	161	15.26	4.91	3.59	1.48	bdl	0.01	2.82	7.18	2.77	113.74
Ho	165	2.19	0.30	0.52	0.13	0.03	0.18	0.51	1.20	0.35	7.83
Er	166	6.32	0.02	0.08	bdl	bdl	bdl	0.17	0.64	0.02	5.27
Tm	169	4.16	0.32	0.33	0.09	0.01	0.07	0.33	0.63	0.12	9.63
Yb	172	55.59	0.58	0.27	bdl	bdl	bdl	0.40	4.49	0.17	106.59
Lu	175	22.83	2.46	1.20	bdl	bdl	bdl	15.53	4.81	0.96	76.62
Pb	208	3658.46	7.05	16.33	3.24	11.56	9.05	172.50	63.95	10.13	250.63
Th	232	0.14	0.09	0.09	0.05	0.09	0.11	1.71	bdl	bdl	0.81
U	238	0.04	bdl	0.07	0.83	3.17	0.03	3.04	0.07	0.17	1.03
La/Nd		3.66	bdl	bdl	0.15	0.06	0.05	0.59	0.67	0.01	1.02
La/Lu		7.19	bdl	bdl	bdl	bdl	bdl	0.41	2.59	0.14	3.05
Ba/Nd		bdl	3.21E+02	8.88E+02	4.09E+03	2.19E+03	4.41E+03	6.12E+03	4.12E+04	2.20E+02	7.33E+03
Th/U		3.73	bdl	1.24	0.06	0.03	3.57	0.56	bdl	bdl	0.79

Table 2 (continued). Analyte concentrations corrected for dilution of samples NY C9 – ARK Linda (ppt)

Element	Atomic Mass	NY C9	Marcellus D27	NY Site B	NY C6	Marcellus D31	NY C21	NY C1	JOS EFF	Marcellus M2	ARK Linda
B	11	13093	14905	10442	27055	10780	159483	41441	18268	33216	64365
Al	27	145.40	221.15	74.07	57.88	270.92	adl	11034.76	adl	172.44	adl
Ca	43	1.13E+08	2.38E+07	3.18E+07	3.65E+07	2.82E+07	1.51E+07	6.50E+07	2.73E+07	2.94E+07	9.94E+04
Sc	45	23.13	1.69	2.74	6.30	3.51	1.27	10.82	2.82	6.17	bdl
Ti	48	644158	163794	228749	286155	209265	103697	466819	188734	214249	491
V	51	bdl	bdl	bdl	bdl	bdl	bdl	bdl	bdl	bdl	bdl
Cr	52	149.15	110.27	178.15	538.82	188.69	60.81	525.39	90.89	89.34	2.49
Fe	54	428179	28012	466305	375991	2134118	44298	2154812	2360	4405594	23
Mn	55	509473	45228	67378	151879	305263	111264	506208	1553	73596	5
Ni	58	3311.08	221.11	3336.27	3126.51	16568.58	316.98	18963.56	3.38	32269.24	bdl
Co	59	23.97	0.26	121.20	121.20	15.25	18.08	243.26	0.60	23.89	bdl
Cu	65	253.38	61.83	23.32	199.26	266.58	184.83	6123.29	26.67	300.17	2.21
Zn	66	7595	4364	2301	18810	1747	605	12472	153	597	223
As	75	128.88	199.35	115.52	201.19	130.62	65.43	52.16	122.08	59.88	8.56
Se	82	38826	bdl	10321	1246	9849	1436	2311	961	19193	748
Ag	109	10.17	0.06	bdl	0.61	1.99	71.17	3.10	0.30	bdl	bdl
Cd	111	230.75	41.28	38.14	76.26	17.65	2403.07	44.91	52.33	50.76	24.24
Cs	133	949.01	187.27	304.42	486.76	363.43	2955.90	405.51	1045.79	132.26	99.84
Ba	135	bdl	107420	16424	65409	3100	664677	253487	80224	6340	21800
La	139	289.69	3.25	5.31	5.87	0.61	1959.56	20.91	1.10	2327.23	bdl
Ce	140	21.19	1.62	7.09	2.83	1.83	322.64	61.31	bdl	8360.68	bdl
Pr	141	4.58	0.37	1.00	0.86	0.58	56.43	7.47	0.32	927.43	0.15
Nd	143	47.75	22.95	10.08	24.11	3.65	974.68	48.80	14.90	3927.90	3.75
Sm	147	172.86	3.15	1.89	2.98	0.43	1025.22	16.92	1.22	443.28	bdl
Eu	153	12398	115	26	52	5	69701	131	47	75	11
Gd	157	416.90	71.35	22.44	18.07	bdl	3623.42	9.61	bdl	520.62	bdl
Tb	159	2.82	0.69	0.94	3.62	bdl	157.74	4.20	0.36	52.49	bdl
Dy	161	42.50	19.42	14.00	18.48	4.54	479.35	20.33	7.49	210.81	1.30
Ho	165	1.72	0.61	0.75	1.43	0.49	24.12	2.42	0.85	33.80	0.32
Er	166	3.86	0.46	0.42	0.73	0.15	31.61	4.82	0.41	150.83	0.07
Tm	169	12.06	0.62	0.41	0.57	0.17	36.00	0.80	0.28	11.11	0.01
Yb	172	214.32	1.49	1.11	1.81	0.48	294.53	5.53	1.08	65.23	0.04
Lu	175	109.57	12.73	9.36	14.04	4.32	1618.10	10.05	7.71	17.44	2.85
Pb	208	3737.60	100.95	380.80	403.01	108.94	950.87	1697.46	24.30	38.35	1.30
Th	232	bdl	bdl	bdl	bdl	bdl	22.88	0.31	bdl	3.39	bdl
U	238	0.28	0.33	0.69	1.19	0.18	26.62	1.13	0.05	0.58	0.67
La/Nd		6.07	0.14	0.53	0.24	0.17	2.01	0.43	0.07	0.59	bdl
La/Lu		2.64	0.26	0.57	0.42	0.14	1.21	2.08	0.14	133.44	bdl
Ba/Nd		bdl	4.68E+03	1.63E+03	2.71E+03	8.50E+02	6.82E+02	5.19E+03	5.38E+03	1.61E+00	5.81E+03
Th/U		bdl	bdl	bdl	bdl	bdl	0.86	0.27	bdl	5.87	bdl

Table 2 (continued). Analyte concentrations corrected for dilution of samples NY C25 – Marcellus D32 (ppt)

Element	Atomic Mass	NY C25	NY Sweezy	NY C20	NY C30	Marcellus D40	NY C28	NY C2	NY C24	NY C8	Marcellus D32
B	11	773401	3820	45019	8342	9531	8148	122334	505554	14199	5123
Al	27	124.51	7606.05	adl	0.75	94.62	adl	490.31	750.54	356.39	adl
Ca	43	3.37E+07	4.34E+06	4.27E+06	8.29E+07	2.10E+07	7.91E+07	4.10E+07	2.82E+07	9.23E+07	2.30E+07
Sc	45	4.88	3.40	bdl	17.43	2.51	16.03	6.92	4.43	17.90	1.92
Ti	48	232263	34922	32092	524335	152618	513901	283798	185374	587427	170895
V	51	bdl	27.77	bdl	bdl	bdl	bdl	bdl	bdl	bdl	bdl
Cr	52	72.05	140.52	75.83	89.96	68.08	20.78	59.74	74.27	620.21	73.22
Fe	54	57622	4412	206	568323	300262	524022	821139	258862	721665	772785
Mn	55	112525	18201	12748	639689	44905	535280	180062	93872	644206	168214
Ni	58	392.70	121.04	62.70	4120.07	2279.29	3808.83	6409.03	1928.87	5366.54	5808.37
Co	59	2.33	83.48	13.70	65.59	0.28	32.82	137.97	6.08	50.06	bdl
Cu	65	66.57	105.60	90.11	144.89	48.05	285.95	4421.10	392.60	269.17	32.16
Zn	66	2324	2806	837	5288	3009	3758	8591	23164	5767	507
As	75	89.74	32.81	5.99	94.22	6801.99	108.71	25.00	13.96	66.70	113.65
Se	82	88486	231	201	27624	191	53011	26779	13411	141655	1367
Ag	109	62.93	0.52	0.34	1.40	bdl	0.95	21.87	73.80	1.26	bdl
Cd	111	2736.78	42.97	32.38	121.64	29.69	97.23	792.48	2463.09	96.47	27.95
Cs	133	14741.51	25.25	767.35	837.74	49.90	832.51	5068.87	14880.17	999.04	168.46
Ba	135	617820	3699	2221	bdl	30813	bdl	18371	138447	bdl	10915
La	139	1212.85	307.17	bdl	271.70	1.74	281.28	492.41	1532.44	332.66	0.47
Ce	140	182.83	240.79	0.04	19.48	1.43	36.20	48.23	373.70	33.84	0.14
Pr	141	40.84	0.85	0.49	4.14	0.40	5.96	10.45	59.55	6.73	0.23
Nd	143	1026.57	13.82	10.20	27.97	17.44	41.76	272.28	1090.01	37.92	9.89
Sm	147	652.71	0.45	0.98	148.93	1.85	156.21	277.51	835.71	188.01	1.88
Eu	153	44953	4	18	11807	49	11182	19642	52271	13494	56
Gd	157	1969.67	bdl	bdl	377.62	37.42	359.61	1355.91	3895.56	444.39	60.45
Tb	159	38.61	0.20	0.34	1.22	0.37	1.98	20.72	61.45	2.30	0.97
Dy	161	368.27	5.20	13.46	30.71	16.35	34.66	300.71	947.50	40.54	21.78
Ho	165	36.23	1.13	1.45	2.01	0.85	1.83	10.72	37.63	1.80	0.59
Er	166	33.20	0.66	0.58	2.56	0.36	2.97	9.71	48.37	2.97	0.38
Tm	169	36.49	0.20	0.44	11.23	0.45	9.60	21.25	57.39	11.59	0.56
Yb	172	547.32	0.64	0.53	201.84	1.65	185.69	247.89	585.01	251.74	1.05
Lu	175	500.87	6.11	11.00	107.29	13.04	114.05	331.91	918.30	139.86	17.80
Pb	208	5854.59	422.99	93.90	1151.18	123.67	654.03	13391.90	23510.93	2489.37	6.42
Th	232	11.63	26.25	bdl	bdl	bdl	bdl	1.07	16.34	bdl	bdl
U	238	8.16	29.95	1.56	0.19	0.97	0.23	3.18	14.03	0.44	0.19
La/Nd		1.18	22.22	bdl	9.72	0.10	6.73	1.81	1.41	8.77	0.05
La/Lu		2.42	50.25	bdl	2.53	0.13	2.47	1.48	1.67	2.38	0.03
Ba/Nd		6.02E+02	2.68E+02	2.18E+02	bdl	1.77E+03	bdl	6.75E+01	1.27E+02	bdl	1.10E+03
Th/U		1.43	0.88	bdl	bdl	bdl	bdl	0.33	1.16	bdl	bdl

Table 2 (continued). Analyte concentrations corrected for dilution of samples NY C3 – NY C17 (ppt)

Element	Atomic Mass	NY C3	Marcellus D37	Marcellus M1	ARK Prince	Marcellus D14	NY C7	NY C27	Marcellus D33	NY Site C	NY C17
B	11	4577	2570	11570	21372	4521	493798	9176	3722	30559	12475
Al	27	adl	110.15	52.41	adl	adl	117.87	30.24	adl	105.10	249.48
Ca	43	1.91E+07	1.41E+07	7.56E+06	9.17E+04	1.63E+07	4.34E+07	7.14E+07	3.28E+07	3.12E+07	3.59E+07
Sc	45	2.32	0.97	bdl	bdl	bdl	9.99	13.91	6.37	7.14	13.99
Ti	48	123159	105726	54107	396	124590	306549	562704	296039	250180	310643
V	51	bdl	bdl	bdl	bdl	bdl	bdl	1.32	bdl	bdl	2.50
Cr	52	33.84	59.25	127.94	26.96	56.95	88.89	103.39	34.03	30.11	79.63
Fe	54	141242	2108	862553	233515	246871	251339	418039	54849	96824	388449
Mn	55	72421	29735	46951	204	34925	67574	647527	65901	104617	139166
Ni	58	1073.88	3.34	5656.03	1630.74	1806.82	2364.39	3429.26	475.98	872.41	3456.63
Co	59	58.89	0.94	10.50	0.55	bdl	31.02	24.28	bdl	1.93	5.86
Cu	65	356.63	86.86	115.26	11.18	72.30	212.86	169.95	522.20	bdl	177.41
Zn	66	11466	4007	1132	277	2198	2683	13154	7141	285	12120
As	75	237.89	32.96	27293.60	34.17	11.84	d.n.r.	d.n.r.	d.n.r.	d.n.r.	d.n.r.
Se	82	28954	21175	1173	bdl	19202	d.n.r.	d.n.r.	d.n.r.	d.n.r.	d.n.r.
Ag	109	bdl	0.10	bdl	bdl	bdl	66.31	1.47	bdl	2.29	0.38
Cd	111	23.10	24.52	17.09	5.69	16.47	2221.05	107.63	32.01	115.15	42.40
Cs	133	143.25	82.77	26.27	14.35	111.24	20526.45	855.81	452.89	1389.75	653.36
Ba	135	377543	4754	51780	11868	41749	183392	bdl	5563	255	939921
La	139	5.70	1.53	1.51	bdl	0.11	1797.57	295.09	4.18	149.49	17.21
Ce	140	0.75	2.13	1.78	bdl	1.51	516.09	27.15	5.20	16.50	6.92
Pr	141	0.38	0.42	0.29	0.08	0.14	59.48	4.41	0.54	2.69	0.62
Nd	143	5.33	9.41	3.97	1.25	1.84	830.01	21.21	11.91	45.82	10.10
Sm	147	3.77	1.71	0.84	0.01	0.20	801.47	139.99	1.56	70.16	10.29
Eu	153	239	38	45	19	32	47005	11507	45	5310	609
Gd	157	25.35	48.19	47.54	33.96	7.06	2993.72	346.94	45.68	263.55	41.11
Tb	159	30.26	0.32	0.02	0.21	bdl	65.85	0.71	0.25	2.67	0.37
Dy	161	13.62	14.92	8.98	3.93	6.77	658.16	27.19	20.89	50.87	17.50
Ho	165	0.51	0.57	0.40	0.15	0.31	41.92	1.36	0.85	1.72	0.69
Er	166	0.27	0.36	0.06	bdl	bdl	33.39	2.52	0.26	1.68	0.65
Tm	169	0.50	0.43	0.35	0.12	0.19	51.02	11.21	0.64	5.55	0.68
Yb	172	2.49	0.84	1.35	0.17	0.50	623.82	216.38	0.73	70.68	5.89
Lu	175	14.13	10.67	6.85	3.73	6.22	674.86	98.19	14.57	57.00	12.34
Pb	208	345.91	40.97	189.90	2.27	107.53	12154.11	2064.10	7.89	50.21	272.14
Th	232	bdl	bdl	bdl	bdl	bdl	6.80	bdl	bdl	bdl	bdl
U	238	1.66	0.11	1.33	0.60	0.03	12.20	0.44	0.05	0.16	0.02
La/Nd		1.07	0.16	0.38	bdl	0.06	2.17	13.91	0.35	3.26	1.70
La/Lu		0.40	0.14	0.22	bdl	0.02	2.66	3.01	0.29	2.62	1.39
Ba/Nd		7.08E+04	5.05E+02	1.30E+04	9.52E+03	2.27E+04	2.21E+02	bdl	4.67E+02	5.58E+00	9.31E+04
Th/U		bdl	bdl	bdl	bdl	bdl	0.56	bdl	bdl	bdl	bdl